

Florida State University Libraries

Electronic Theses, Treatises and Dissertations

The Graduate School

2021

Monitoring Peptide Secretion Dynamics from Human Pancreatic Cells Using a Sandwich Assay and Microfluidics

Wesley James Eaton

FLORIDA STATE UNIVERSITY
COLLEGE OF ARTS AND SCIENCES

MONITORING PEPTIDE SECRETION DYNAMICS FROM HUMAN PANCREATIC CELLS
USING A SANDWICH ASSAY AND MICROFLUIDICS

By

WESLEY JAMES EATON

A Dissertation submitted to the
Department of Chemistry and Biochemistry
in partial fulfillment of the
requirements for the degree of
Doctor of Philosophy

2021

Wesley Eaton defended this dissertation on November 15, 2021.

The members of the supervisory committee were:

Michael G. Roper
Professor Directing Dissertation

Steven Lenhart
University Representative

Geoffrey F. Strouse
Committee Member

Scott M. Stagg
Committee Member

Robert A. Lazenby
Committee Member

The Graduate School has verified and approved the above-named committee members, and certifies that the dissertation has been approved in accordance with university requirements.

This dissertation is dedicated to my parents, Kevin and Leda Eaton

ACKNOWLEDGMENTS

I want to thank everyone in my life who has provided me with their support and love throughout my graduate studies. First and foremost, my deepest gratitude goes to my advisor, Dr. Michael Roper, who believed in me and took a chance letting me join his research group as an undergraduate at Florida State. Thank you for your patience and guidance and continuous support throughout. You are a role model as a scientist and as a person that I strive to be more like.

Next, I'd like to extend a special thanks to my doctoral committee members Dr. Steven Lenhart, Dr. Geoffrey F. Strouse, Dr. Scott M. Stagg, and Dr. Robert A. Lazenby, for their time, support, and guidance with my research. Thank you to Florida State University, the Department of Chemistry and Biochemistry and all the staff that support the department.

I also want to thank current and former lab mates from the Roper lab for their camaraderie and mentorship throughout the years. I am grateful to have worked with many smart and hardworking people who are eager to learn and teach. Thank you to Nick Mukhitov, Basel Bandak, Kim Evans, Rafael Masitas, Joel Adablah, Weijia Leng, Anna Adams, Matt Donohue, Rob Filla, Yao Wang, I An Wei, Damilola Adeoye, Emmanuel Ogunkunle, Valerie Zaffran and Daniel Steyer – I am blessed to have had the opportunity to work alongside great peers and friends during my graduate career.

I am fortunate to have an incredible family to support me. To my parents Kevin and Leda Eaton, and to my siblings Allie, Lindsey, and Cameron; thank you for your love and encouragement, you mean the world to me, and I could not have done this without you. Thank you to Sydney Niles for your continued support and love.

TABLE OF CONTENTS

List of Tables	vii
List of Figures.....	viii
Abstract.....	xii
CHAPTER 1 – INTRODUCTION	1
Type II Diabetes in Humans.....	1
Glucagon and Insulin for Blood Sugar Regulation	1
Islets of Langerhans.....	2
Pancreatic Cells and Endocrine Function.....	2
Glucagon Physiology and Action.....	3
Previous Measurement of Glucagon with Immunoassays	5
Forster-Resonance Energy Transfer (FRET) Assay for Insulin and Glucagon Measurements .	6
Dissertation Overview	8
CHAPTER 2 - A MICROFLUIDIC SYSTEM FOR MONITORING GLUCAGON SECRETION FROM HUMAN PANCREATIC ISLETS OF LANGERHANS.....	10
Introduction.....	10
Methods and Materials.....	11
Results.....	15
Conclusions.....	24
CHAPTER 3 - AN AUTOMATED SYSTEM FOR LOW VOLUME MEASUREMENT OF GLUCAGON AND INSULIN FROM HUMAN PANCREATIC ISLETS OF LANGERHANS	25
Introduction.....	25
Methods and Materials.....	26
Results.....	31
Conclusion	38
CHAPTER 4 – SUMMARY AND FUTURE DIRECTIONS.....	40

Summary	40
Future Directions	40
APPENDIX A - SIMULTANEOUS MEASUREMENTS OF REACTIVE OXYGEN SPECIES (ROS) WITH INSULIN SECRETION FROM ISLETS OF LANGERHANS	44
APPENDIX B - DEVELOPMENT OF A CUSTOM OPTICAL SYSTEM FOR INSULIN MEASUREMENT FROM A SINGLE ISLET OF LANGERHANS	47
APPENDIX C - ABBREVIATIONS	54
APPENDIX D - ANIMAL CARE AND USE COMMITTEE ASSURANCE LETTER	55
References	56
Biographical Sketch	64

LIST OF TABLES

2-1 Donor characteristics for human islets.	12
2-2 Model parameters for the finite element simulation.....	14
3-1 Donor characteristics for human islets.	27

LIST OF FIGURES

- 1-1 Fluorescence microscopy of frozen islet sections stained to reveal hormone spatial information in islet cells. Insulin (red) present in cells is shown on the left with somatostatin and glucagon both labeled with a green dye, FITC (Fluorescein isothiocyanate), being middle and right, respectively. (Obtained with permissions)3
- 1-2 Jablonski diagram illustrating FRET process (left) and absorption and emission spectra of a donor-acceptor pair (right). (obtained with permissions)6
- 1-3 FRET sandwich assay diagram illustrating the antigen complex increased FRET efficiency. When the donor and acceptor are far apart the distance between the two fluorophores is much greater than R_0 , this results in a low FRET efficiency. At the bottom of the figure, when the antigen complex formed the fluorophores are in close proximity and increase FRET efficiency.....7
- 2-1 Calibration of TR-FRET assay. A representative calibration of the TR-FRET assay is shown. The points are the average of 3 replicates and the error bars are ± 1 standard deviation. The inset shows the lower region of the curve. The plot was fit with a linear regression line $y=2.6659x$ ($r^2 = 0.999$).....16
- 2-2 Microfluidic system. (A) A 3D drawing of the PDMS/glass microfluidic device used in this report. The outputs of two syringe pumps were coupled at a tee (not shown) and input into the inlet port of the device. Islets were loaded through the central loading port and covered with a piece of PCR film. Tubing at the outlet (not shown) was used to collect fractions of the perfusate every 2 min. (B) An image of the microfluidic device loaded with human islets was used to mimic the placement and size distribution in a finite element model. (C) The picture in (B) was used to build a finite element model of fluid flow in the device. The image is from the simulation and shows a composite view from a slice of the fluid velocity taken in the middle of the channel and a surface plot of the shear stress on the islets. The scale bar at the bottom of the image is for both the fluid velocity and shear stress. The range for shear stress is 0.0–75 mPa, and the range for velocity is 0.0– 1.25 mm s⁻¹17
- 2-3 Flow dynamics. Low (0 pg mL⁻¹) and high (1200 pg mL⁻¹) glucagon concentrations were delivered to the device through the syringe pumps in a pattern shown by the red line (corresponding to the right y-axis). The flow through the device was fractionated every 2 min and measured using the TR-FRET assay. The amount of glucagon in each fraction is shown by the data points and corresponds to the left y-axis.....18
- 2-4 Control experiments. 25 islets from Donor 5 were exposed to a constant 20 mM glucose for the duration of the experiment. At 10 and 40 min, the flow rates from the two syringe pumps were switched to mimic the experiment for initiating glucagon release (for example, the experiment shown in Figure 2-3).....19
- 2-5 Representative glucagon secretion profiles. In both traces, the measured glucagon levels are shown by the black points and correspond to the left y-axis, while the glucose profile

delivered to the device is shown as a red line and corresponds to the right y-axis. (A) A representative trace from a group of 30 islets from donor 4 that released in a “burst” pattern. (B) A representative group of 45 islets from donor 4 that released glucagon in a “sustained” pattern20

2-6 All glucagon secretion profiles are shown where the total glucagon content from the islets were assayed after the experiment. The number of islets and donor for each panel were: **A)** 30 islets, donor 4 (burst), **B)** 20 islets, donor 4 (burst); **C)** 30 islets, donor 4 (burst); **D)** 45 islets, donor 4 (sustained); **E)** 30 islets, donor 3 (burst); **F)** 25 islets, donor 3 (sustained); **G)** 28 islets, donor 3 (no response); **H)** 25 islets, donor 5 (burst).....21

2-7 Average glucagon levels. The total glucagon secretion levels normalized over the collection time (total glucagon min⁻¹) for all traces shown in Figure 2-6 were averaged and shown as a function of glucose level. The difference in the amount of glucagon released during 1 mM glucose was significantly higher than that at 20 mM glucose (p = 0.002, 1-tailed Student's t-test). Average is shown as the thick horizontal line with error bars equal to +/-1 standard deviation.....22

2-8 Additional glucagon secretion profiles. Shown are additional experiments that were performed on batches of islets, but the islets were not collected after the experiment. These are provided to show more of the profiles but were not included in the data shown in Figure 2-5. (A-C) donor 1; (D-E) donor 2. The secretion values were not normalized to the islet number, and the islet number is given in the y-axis23

3-1 Microfluidic device design. A 2D display of the microfluidic device design, includes two inlets to allow for a dual perfusion of buffers to the islets chamber, where the islets are loaded and remain during an experiment. The mixing junction joins the fluid streams from the two inlets, and the serpentine channel design after the mixing cross allow for the fluid stream to be homogenized prior to the islet chamber. The outlet directs fluid flow to the fraction collection system.27

3-2 Diagram of capillary depositing sample into well with oil layer and the subsequent splitting of the sample29

3-3 Comparison of assay signal of glucagon calibration incubated with layer of light mineral oil. Each assay was repeated in triplicate, and both were incubated with a PCR cover on the same low volume well plate. After 12-hour incubation the TR-FRET value were measured and reported as a ratio for each concentration.....32

3-4 Insulin and glucagon TR-FRET assay calibrations. **(A.)** A representative of the insulin TR-FRET calibration is shown and **(B.)** a representative TR-FRET calibration of glucagon is shown. The points in both are an average of three replicates and the error bars are ± 1 SD.33

3-5	Flow dynamics. Dual perfusion system where blue indicates the level of glucagon and red the level of insulin being flowed into device by pressure system. White section is 100% glucagon and 0% insulin, grey is 100% insulin and 0% glucagon.....	34
3-6	Human islet traces with dual peptide detection. Two traces are shown from a batch of human islets, while detecting both insulin and glucagon. The y-axis is the percent released of each, the total secreted measured and the total remaining in the islets after contributing to the percent value. The white section of the trace has a glucose value of 5.6 mM and the grey section has a glucose value of 16.7 mM. 30 islets were used for both traces shown.	35
3-7	Human islet traces with dual peptide detection and dynamic glucose perfusion. The trace shown is from batch human islets (30 islets) in a microfluidic device. The y-axis is the percent released of each, the total secreted measured and the total remaining in the islets after contributing to the percent value. Glucose was delivered in a staircase fashion at 1, 5, 10, 15 mM and ending at 20 mM before returning down to 1 mM. Each concentration was held for 9 minutes so that three fractions could be collected during all intervals.....	36
3-8	The total glucagon (blue) and insulin (red) secretion levels normalized over the collection time (total glucagon or insulin min ⁻¹) for both traces shown in Figure 3-6 (left). Average secretion levels normalized over collection time for glucagon and insulin are shown (middle and right) over a glucose staircase dose delivery from Figure 3-7.....	38
4-1	The custom optical system assembled to make FRET measurements. (A.) The LED and collimator obtained from Thorlabs was controlled by a time to live signal outputted from a DAQ card connected to LabView. The light is collimated and directed into a dichroic mirror and up through the back of the 40x Nikon objective. Fluorescence is then collected by epifluorescence and directed towards the photon measuring system (B.) The collected light is passed through an iris and emission filters before the photomultiplier tube.....	41
4-2	Glucagon positive control test. The right axis corresponds to the quantum dot signal during the off cycle of the LED. The left axis corresponds to the glucagon 0 nM and 10 nM standard solutions used to test the TR-FRET measurement of the system	42
A-1	H ₂ O ₂ -induced increases in Grx1-roGFP2 fluorescence. Five biosensor-expressing islets were held in a glass-bottomed dish containing BSS with 3 mM glucose. Fluorescence was measured from the biosensor every 10 s and is plotted on the left y-axis. H ₂ O ₂ was spiked into the dish to a final concentration of 10 μM at the time indicated by the horizontal bar.	45
A-2	Acute delivery of 11 mM glucose. Grx1-roGFP2-expressing islets were initially perfused with 3 mM. The glucose concentration was increased to 11 mM during the time shown by the horizontal bar on the tops of the figures. The glucose level was returned to 3 mM for the final 10 min of recording.	46
B-1	(A) Schematic of a wide field epifluorescence microscope, where one microscope objective is used for sample illumination and detection. The purple and green light trace represent excitation light that is scattered back through the objective and read by the detector. (B)	

Schematic of a confocal microscope. The focusing lens completes the confocal geometry to selectively image a single point within a thick sample.....48

B-2 Schematic of the detection system for laser induced fluorescence adapted. The red lines represent the path the laser light takes to the microfluidic device and the fluorescence path from the separation channel to the photomultiplier tube49

B-3 Microfluidic device design incorporates two different flow components. The black line represent channel where gravity driven flow occurs. The red line shows where electroosmotic flow drives the liquid from the grounded inlets to the -5000 V waste outlet.50

B-4 A electropherogram comparison between a wide field (black) measurement and a confocal measurement (red)51

B-5 An insulin competitive immunoassay calibration curve, increasing the amount of insulin consequently decreases the amount of insulin-cy5 that is bound to the antibody. There is an inverse relationship between the B/F ratio and insulin concentration (nM).....52

B-6 Single islet insulin detection using confocal system. The separation immunoassay was used in a competitive format. Glucose stimulation was from 3 mM to 11 mM for 45 min and back down to 3 mM.....53

ABSTRACT

Type II diabetes is a leading cause of death in the United States due to its high prevalence in adults with high blood pressure, obesity, other health problems. It affects ~10.5% of the U.S population, and this number continues to increase every year (projected to reach over 30% by 2050). Diabetes affects blood sugar regulation due to dysfunction in release patterns for insulin and glucagon. Currently, medication exists to help manage glucose concentrations in the body; however, no “cure” exists and much remains unknown regarding how processes go awry in a diabetic state. Specifically, a healthy human body releases insulin and glucagon in an oscillatory pattern into the bloodstream in response to meals and periods of fasting to control blood glucose levels. However, in people with diabetes, the release of these hormones is disrupted, which can lead to a variety of symptoms and risk factors including seizures and death. The first steps in developing better therapeutics for people with diabetes is understanding the complex hormone release patterns in healthy human bodies as well as characterizing the disrupted release patterns in people with diabetes.

Microfluidic devices have been introduced to characterize small concentrations of analytes (e.g., hormones) in liquid due to their ability to employ low-volume flow rates in highly controlled environments. Additionally, microfluidics can be coupled with highly sensitive immunoassay-based optical measurement systems to detect low concentrations of diabetes-related hormones such as insulin and glucagon. Microfluidics presents an unparalleled strength for understanding cellular function and communication because it allows determination of concentration changes for insulin and glucagon over very short time periods (e.g., 2-5 minutes), which gives insight into real-time hormone release within the body. The work described herein employs microfluidics coupled to various analytical techniques to study glucagon and insulin release from healthy human pancreatic cells and provide increased understanding regarding their release patterns.

Chapter 1 presents an introduction to the physiology and function of pancreatic cells in the human body and explains how immunoassay techniques are employed for characterization of pancreatic hormones. Chapter 2 introduces a novel microfluidic system to study glucagon secretion from human pancreatic cells using a Förster -resonance energy transfer (FRET)-based assay, which provides temporal resolution for glucagon release traces from ~30 islets. Finally, Chapter 3 builds upon the previous chapter and provides a method to simultaneously detect insulin and glucagon

released from pancreatic cells in real time to characterize the release relationship of the two hormones.

CHAPTER 1

INTRODUCTION

Type II Diabetes in Humans

The human endocrine system is equipped with an organ called the pancreas, which regulates blood sugar and aids in digestion.¹ In healthy adults, blood sugar patterns are oscillatory² and controlled through release of the hormones insulin and glucagon from the pancreas;³ these hormones lower and raise blood sugar levels to maintain healthy blood glucose levels.⁴ However, in people with type II diabetes, this release pattern is disrupted,⁵ which can result in unsafe blood sugar levels.⁶ Additionally, co-symptoms such as fatigue, pain, and nausea accompany unregulated blood sugar levels, and extreme cases of unregulated glucose can lead to more serious complications including death.⁷ Abundant studies report the connection between excessive sugar intake and the development of type II diabetes.^{4,8,9} However, it is unclear how exactly blood sugar regulation becomes disrupted. Furthermore, much remains unknown regarding the release patterns of insulin and glucagon in healthy humans. Additionally, the oscillatory release of these hormones occurs over very short time periods (as low as 2 minutes), which presents a unique challenge for characterization of the release profiles.¹⁰⁻¹² Thus, additional studies are required to characterize the release of these hormones on short time scales.¹²

Glucagon and Insulin for Blood Sugar Regulation

To synthetically control blood sugar, people with diabetes typically inject insulin, which lowers blood sugar.¹³ However, insulin can be costly, and injections are tedious.¹⁴ As previously mentioned, glucagon and insulin are hormones released by the pancreas to maintain healthy blood glucose levels.¹³ Specifically, in healthy humans, blood sugar rises after a meal is consumed, and insulin is released to lower blood sugar.¹⁵ Conversely, during a period of fasting, blood sugar levels drop, and glucagon is released to raise blood sugar.⁴ However, people with disrupted blood sugar regulation experience hypo- and hyperglycemia,¹⁶ which occurs when blood sugar levels are too low or too high, and insulin/glucagon release does not occur normally to maintain healthy blood sugar levels.^{9,13,17} Specifically, hypoglycemia is a low period of blood sugar level outside of a normal range; this causes confusion, blurred vision, and seizures, along with a long list of other

symptoms.¹⁸ Severe hypoglycemic episodes are used as a mortality predictor in patients with diabetes. Conversely, hyperglucagonemia (high glucagon levels) is usually observed in diabetic patients when the body fails to respond appropriately to high glucose levels.^{13,19,20}

Islets of Langerhans

As previously mentioned, the pancreas is the organ responsible for blood sugar regulation because pancreatic endocrine tissue secretes the hormones insulin and glucagon, which lower and raise blood glucose levels to keep it within a healthy range.²¹ Despite this key role in blood sugar regulation, the endocrine portion of the pancreas accounts for only 1-2 wt%, whereas exocrine and vascular tissue make up the remaining 98-99 wt%.

Clusters of cells are scattered throughout the pancreas and are known as islets of Langerhans. First discovered in 1869 by Paul Langerhans, the cell clusters were named “islets” because they resembled islands in the pancreas.²² Each islet is comprised of ~2000-3000 cells and there are about 1 million islets found in the human pancreas.^{10,23–25} Pancreatic islets release signaling peptide hormones in unison. These two processes are oscillatory and drive cellular communication throughout the body.²⁶ Additionally, the pancreas also aids in digestion and absorption of macronutrients in food, including proteins, fats, and carbohydrates through the release of enzymes from the pancreatic duct.²⁷

Pancreatic Cells and Endocrine Function

Islets are comprised of four major cell types: alpha, beta, delta, and gamma and epsilon cells. Alpha cells, which make up between 10-65% of the endocrine cells in human islets,²⁸ synthesize and secrete glucagon into the liver by means of the bile duct to initiate the process of gluconeogenesis and glycogenolysis.²⁹ These two processes are responsible for increasing blood glucose levels by acting on hepatocyte cells in the liver.³⁰

Beta cells synthesize insulin, which signals the liver to lower blood sugar levels upon secretion. Insulin regulates metabolism by inducing the uptake of nutrients from blood into skeletal muscle cells and other peripheral cells and reducing the sugar output of the liver. Elevated insulin levels in the bloodstream have effects on a wide variety of protein synthesis mechanisms. Additionally, beta cells make up the largest portion (28-75%) of the endocrine cells in human islet of Langerhans and are the only cells in mammals which can produce insulin.²⁸ When there is a

spike in blood glucose levels, beta cells respond by causing exocytosis of insulin-carrying vesicles, which releases insulin into the bloodstream.³¹ This is known as glucose-stimulated insulin release (GSIS), and the process is imperative for lowering blood sugar in the human body after a meal. Delta cells are also found in pancreatic islets but make up a smaller portion of the total cells (1.2-22%).²⁸ These cells produce somatostatin, which acts as an inhibitor to stop various hormonal processes, such as insulin and glucagon secretion when the hormone levels become too high.³²

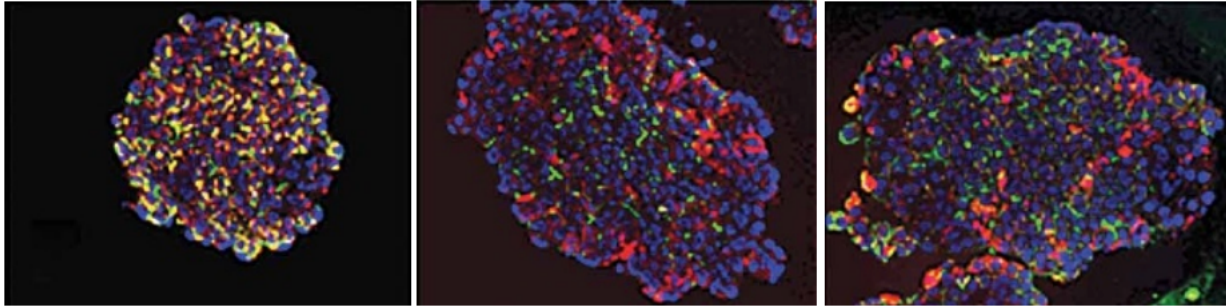


Figure 1-1. Fluorescence microscopy of frozen islet sections stained to reveal hormone spatial information in islet cells. Insulin (red) present in cells is shown on the left with somatostatin and glucagon both labeled with a green dye, FITC (Fluorescein isothiocyanate), being middle and right, respectively. (Obtained with permissions)

The final cells that make up pancreatic islets are gamma cells and epsilon cells; gamma cells are 3-5 wt% of the islet whereas epsilon cells make up less than 1 wt% of the total cells. Gamma cells and epsilon cells secrete pancreatic polypeptide and ghrelin respectively. Pancreatic polypeptide regulates other cells in the pancreas and ghrelin has been seen to stimulate hunger when secreted. Both play minor roles in glucose homeostasis relative to insulin and glucagon.

The beta cell content in human islets has been reported to be between 28-75%;²⁸ larger islets (greater than 2000 cells) have the lowest percentage of beta cells. It was found that like-cells (e.g. two beta cells) favored cell connecting adhesions and were stronger than those between two different cell types. Beta cells grouped up with beta cells preferentially, this leads to a somewhat organized structure to the islet, that differs from what a randomly constructed islet would look like.³³

Glucagon Physiology and Action

Glucagon is a peptide composed of 29 amino acids, with an atomic mass of 3485 Dalton.^{10,34,35} The glucagon gene codes to produce proglucagon, which is then cleaved into smaller peptides, one of which is glucagon.^{34,35} Production of glucagon in alpha cells is constant

unless otherwise suppressed, meaning there is no stimulus to glucagon production but can be inhibited by other factors.³⁶ However, glucagon is not secreted from alpha cells unless it is stimulated.³⁶

As previously discussed, alpha cells release glucagon when the blood sugar levels in the body are too low, which raises blood sugar levels by two pathways: glycogenolysis and gluconeogenesis.^{9,29,36} Disruption in these glucagon-signaling processes can lead to hypoglycemia and hyperglucagonemia.³⁷ Hyperglucagonemia is a period when glucagon secretion should be suppressed from alpha cells; the levels of glucagon released can be 4-5 times the normal level.¹⁹ In addition to behavior in patients with diabetes, this also can indicate the presence of alpha cell tumors in the pancreas.³⁸

Glycogenolysis is an important process for raising blood glucose in the human body, and is initiated by glucagon.^{8,39,40} Glycogenolysis provides energy to most cells in the body between meals. Specifically, glycogenolysis involves the breakdown of glycogen (a biopolymer chain made up of 60,000 glucose residues) to release energy in the body.⁴⁰ During a fasting state, pancreatic alpha cells secrete glucagon and initiate glycogenolysis in liver hepatocyte cells; this upregulates enzymes that depolymerize glycogen to allow hepatocytes to secrete glucose and raise blood sugar.^{8,39,41} The first enzyme, glycogen phosphorylase, employs the phosphorylation of alpha (1,4) linkages to yield a glucose 1-phosphate product. The second enzyme, phosphoglucomutase, is responsible for the transition of glucose 1-phosphate to glucose 6-phosphate. Finally, the phosphate group is removed by hexokinase and glucose is circulated in the bloodstream. This is a catabolic process that requires less ATP than its glucose synthesizing counterpart, gluconeogenesis.^{4,8,9,13}

Gluconeogenesis is another chemical process that produces extracellular glucose; however, unlike glycogenolysis, it uses amino acids and lactic acid as precursors for production of glucose. Additionally, gluconeogenesis can be thought of as the reverse reaction of glycolysis, which breaks down glucose in the body to generate two three-carbon compounds and release energy. Gluconeogenesis is initiated during a carbohydrate starvation phase when blood glucose levels are low and less available to be metabolized. Like glycogenolysis, gluconeogenesis is an anabolic process that primarily occurs in the liver.⁴² In addition to production of glucose in the liver, during phases of extreme glucose consumption by skeletal muscles and other tissue, gluconeogenesis can also produce glucose locally where needed.⁴² Glucagon is in a negative

feedback loop with blood glucose; when blood glucose is low, glucagon is secreted into the liver to increase glucose levels. Once glucose levels reach an acceptable level, the secretion of glucagon is halted. It has been shown that controlled glucagon secretion can regulate glucose levels in diabetic patients. Controlling these two processes by glucagon regulation will benefit the development of diabetic therapeutics. Thus, there is a need for sensitive analytical tools to measure glucagon levels from small batches of islets to improve understanding about secretion dynamics of glucagon. Furthermore, the ability to measure glucagon from a single islet does not exist.²⁵ Single islet detection can provide insight about secretion dynamics or frequencies that are not observable when multiple islets are present.¹²

Previous Measurement of Glucagon with Immunoassays

The concentrations for many peptides and peptide fragments that are relevant to understanding diabetes (e.g., insulin and glucagon) can be measured by immunoassays. Specifically, affinity assays such as enzyme linked immunosorbent assay (ELISA) or radioimmunoassay (RIA) have been employed for diabetes research.⁴³ Affinity assays involve the selective binding of an affinity probe (P), typically an antibody, to a probe target (T). The affinity probe target (P-T) complex is then measured and quantified by a detection method. The detection methods for these assays are often spectroscopic and utilize substrate color changes, fluorescence, or chemiluminescence. RIAs require a radiolabel tagged to an antibody. Excess radiolabeled antibody is washed away and the radioactivity (signal) is recorded by a gamma counter. Therefore, they are very sensitive because background radioactive is very low. ELISA involves creating a P-T complex bound on the surface and measuring the enzyme product turnover in solution. A commercial ELISA for glucagon reports a 2.61 pg ml^{-1} detection limit and commercial RIA reports a detection limit of 44 pg mL^{-1} . These low detection limits are useful for diabetes research because insulin- and glucagon-specific antibodies exist to measure the amount of insulin and glucagon released from pancreatic islets.

In addition to traditional assay techniques, affinity probe capillary electrophoresis (CE) coupled with laser induced fluorescence detection has been demonstrated to be an effective alternative for insulin and glucagon measurements.^{12,44,45} CE is used to separate species based on electrophoretic mobility which is related the charge and the hydrodynamic radius of the species. High voltages can be used with small capillaries ($< 20 \text{ }\mu\text{m}$ diameter) for fast dissipation of joule heating, which results in fast and reproducible separations. Fast separations also increase sample

throughput and can be used for monitoring applications such as measuring insulin release pattern from a single islet. Glucagon has been quantified by separation assay from islets using CE; this method was found to have a Limit of detection (LOD) of 3 nM glucagon.¹⁰

In addition to affinity assays and CE, aptamer-assays are also growing in popularity for measurement of peptides and proteins. Aptamers are short, single-stranded RNA or DNA molecules that selectively bind to specific molecules (e.g., peptides). Due to the availability of aptamers that selectively bind to insulin and glucagon, the use of aptamer-based assays are a viable option for measurement of these hormones. These assays have a relatively low dissociation constant and are commonly used in a non-competitive approach, where the aptamer, in high concentration, will chelate the analyte in solution. Methods have been developed using CE to measure glucagon by use of a mirror image aptamer to create an aptamer-glucagon complex, reporting a 40 pM limit of detection for glucagon.

Förster-Resonance Energy Transfer (FRET) Assay for Insulin and Glucagon Measurements

Homogeneous assays utilize the “add and read” approach because they do not require laborious separation steps such as washing, filtration, centrifuging, or magnetic partitioning. A homogeneous assay was employed in Chapter 2 for measurement of glucagon released from pancreatic islets and Chapter 3 for measurement of glucagon and insulin released from pancreatic islets. This assay allows for the detection of glucagon and insulin through a homogeneous Förster -resonance energy transfer (FRET) assay while only requiring low sample volumes, compatible with perfusion experiments.⁴⁶

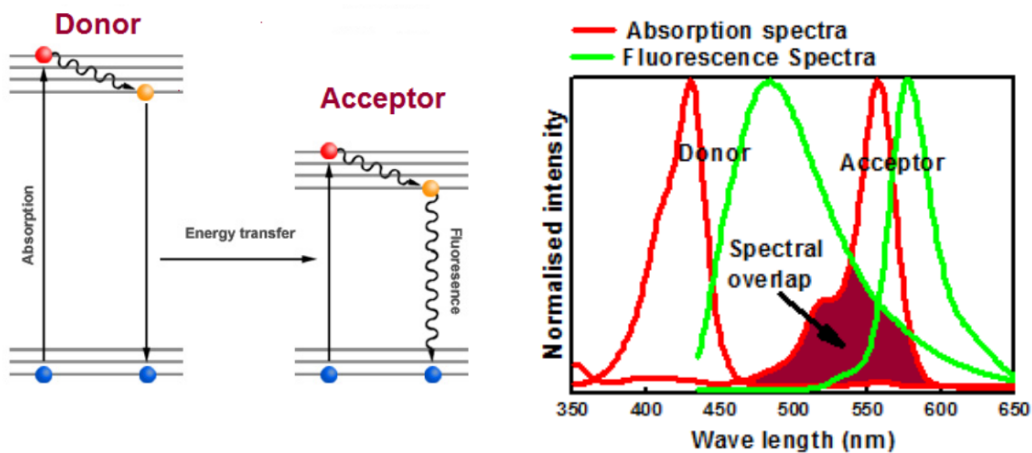


Figure 1-2. Jablonski diagram illustrating FRET process (left) and absorption and emission spectra of a donor-acceptor pair (right). (obtained with permissions)

FRET was first discovered by Theodor Förster in 1946, who found that energy transfer occurred between two fluorophores in close proximity to each other (~1 to 10 nm).^{46,47} Specifically, Förster reported that FRET is a distance-dependent radiationless transfer of energy from an excited donor fluorophore to a compatible acceptor fluorophore.^{47,48} A donor-acceptor pair must have spectral overlap between the donor emission and the acceptor excitation spectrum for FRET to occur (**Figure 1-2**).⁴⁶⁻⁴⁸ FRET efficiency (E_{FRET}) is a function of the inverse sixth power of the distance of the donor-acceptor pair (r) and is expressed in Equation 1. R_0 is the Förster radius at which half of the excitation energy of the donor is transferred to the acceptor, making the efficiency of energy transfer 50%.⁴⁷⁻⁴⁹

$$E_{FRET} = \frac{R_0^6}{(R_0^6 + r^6)}$$

Equation 1-1. The FRET efficiency is expressed as a function of distance between fluorophores. Where E_{FRET} is the probability that an energy transfer event will occur, R_0 is the distance at which efficiency is 50% and r is separation distance.

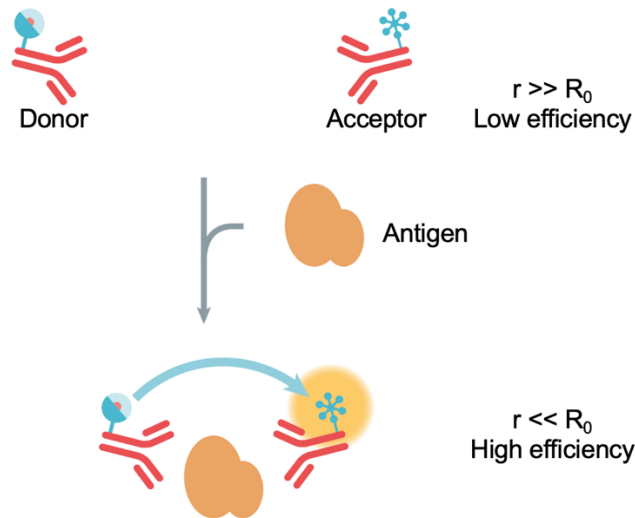


Figure 1-3. FRET sandwich assay diagram illustrating the antigen complex increased FRET efficiency. When the donor and acceptor are far apart the distance between the two fluorophores is much greater than R_0 , this results in a low FRET efficiency. At the bottom of the figure, when the antigen complex formed the fluorophore are in close proximity and increase FRET efficiency.

FRET is a distance dependent process. The donor and acceptor are far apart the FRET efficiency is very low, virtual no FRET occurs demonstrated at the top of **Figure 1-3**. Antigen is solution creates a two-antibody complex bring the donor and acceptor in close proximity increasing FRET efficiency.

Homogenous time resolved Förster resonance energy transfer (TR-FRET) allows for sensitive measurements of homogenous systems. This is utilized in sandwich assays that allow for two antibodies to bind to a specific epitope of an antigen creating a donor-antigen-acceptor complex, where the donor and acceptor have a high FRET efficiency. FRET signal is photon measurements by a photomultiplier tube from both the donor and the acceptor fluorophore; the donor signal is inversely proportional to the acceptor signal. These two values are expressed as a ratio, acceptor signal divided by donor signal, to give quantitative information. This technique is very sensitive because there is a very low false positive rate, because both antibodies need to be bound to the antigen.

An additional way perform to FRET is measure the signal in a time-resolved fashion through use of a donor fluorophore with a long fluorescence lifetime (> 100 s of μ s), which gives us an LOD of 5 pg mL^{-1} for glucagon. When sample is exposed to a pulse of light and then waiting for a period of 100μ s before detection, only FRET emission is detected. This is because all transient fluorescence signal (e.g., scattered excitation light and non-FRET emission) will have decayed to a ground state. The reduction in signal from non-FRET sources during detection enables ultra-sensitive assay readings (as low as 10^{-12} molar), which are ideal for analysis of trace amounts of glucagon and insulin.

Dissertation Overview

The release of glucagon from alpha cells in the islets in response to low blood glucose levels is crucial as its function as a gluco-regulatory hormone. Impairments in the release of glucagon and the inability to regulate blood glucose levels signals traits for diabetes. It is important to develop techniques to measure glucagon release from pancreatic tissue to better understand how the release pattern is affected in the diabetic state. This work focuses on the measurement of gluco-regulatory hormones, glucagon, and insulin, from human pancreatic islets of Langerhans. The objective was to develop a microfluidic device that could house the islets in viable conditions and deliver a dynamic stimulus by perfusion to the cells while collecting the perfusate for analysis, presented in **Chapter 2**. This system was then improved using a new flow control system and

fraction collection was automated using a CNC (computer numerical control) machine and a low volume well plate. Lastly the system was then used to collect a larger fraction over a longer time allow for sample to be split and assayed for two separate hormones presented in **Chapter 3**. Conclusions and future work are presented in **Chapter 4**.

CHAPTER 2

A MICROFLUIDIC SYSTEM FOR MONITORING GLUCAGON SECRETION FROM HUMAN PANCREATIC ISLETS OF LANGERHANS

Introduction

Glucagon is a 29-amino acid hormone peptide derived from proglucagon that acts to increase blood glucose levels by initiating glycogenolysis and gluconeogenesis in the liver.^{1,19} As such, it acts as a counter regulatory hormone to insulin, and is essential for maintaining euglycemia during times of fasting. Glucagon is released from α -cells located in pancreatic islets of Langerhans. In human islets, α -cells make up 5–10% of the islet, with the insulin-secreting β -cells making up 70–80%.⁵⁰ In type 2 diabetes, hyperglucagonemia is often observed,^{1,19} compounding the difficulties of glucose regulation. Despite the importance of glucagon, numerous questions exist into the mechanisms that govern its release.^{1,19,51}

Difficulties associated with measuring glucagon from islets in a time-resolved fashion hamper this understanding. A common way to measure glucagon secretion includes perfusion of a batch of islets followed by fraction collection of the perfusate and subsequent hormone quantitation performed with an enzyme-linked immunosorbent assay (ELISA) or radioimmunoassay.^{17,52} To increase automation and use fewer islets so that the dynamics of secretion can be observed, microfluidic devices have been widely implemented for in vitro cellular studies.^{53,54} These systems have been used in a number of studies with islets of Langerhans for improved control of dynamic conditions compared with traditional methods.^{10,11,44,55–61} Microfluidic devices provide a controlled cellular environment, easy fluid manipulation, automation, and low dilution connections; combined, these factors can lead to high temporal resolution measurements. For example, a microfluidic system was used to perfuse islets and “pseudoislets” to examine differences in secretion profiles of insulin and glucagon using an offline radioimmunoassay.⁶¹ In another example, an electrophoretic immunoassay was used to measure glucagon secretion online from 10 murine islets in response to a change in glucose from 16 to 1 mM.¹⁰ Although electrophoretic immunoassays have been widely used to measure insulin release from islets within microfluidic systems,^{11,12,44,54,57,62} they have not been reported as often with glucagon. We have developed a noncompetitive assay for glucagon using an aptamer,⁶³ but a

complicated fabrication procedure of the necessary microfluidic system limits the widespread applicability of the system.⁶⁴

The previously-described methods employ heterogeneous assays that require separation of the bound and free components; conversely, homogeneous assays do not require a separation step and have been developed for insulin^{65,66} and other peptides⁶⁵ released from islets; one example is a time-resolved Förster resonance energy transfer (TR-FRET) based assay for glucagon. The TR-FRET assay has a 2 pg mL⁻¹ reported limit of detection, which would enable glucagon release from only a few islets to be quantified, possibly allowing release dynamics to be observed.

In this report, we describe initial steps towards the implementation of this TR-FRET assay into a microfluidic based system. A relatively simple microfluidic system is used to house 10–25 human islets and glucose is perfused at varying levels to stimulate glucagon release. Fractions from the perfusate are collected every 2 min and glucagon release is quantified using the TR-FRET assay. We anticipate that the simplicity of the setup combined with the high sensitivity of the assay will enable multiple researchers to use this platform for gaining insight into glucagon secretion dynamics, which could in turn lead to better understanding of type II diabetes and further the development of improved therapeutics.

Methods and Materials

Chemicals and Reagents

Polydimethylsiloxane (PDMS) prepolymer (Sylgard 184) was obtained from Dow Corning (Midland, MI). Dextrose was obtained from Fisher Scientific (Pittsburgh, PA). The TR-FRET glucagon assay was obtained from Cisbio (Waltham, MA). All other reagents were purchased from Sigma-Aldrich (St. Louis, MO) unless noted otherwise. All solutions were made with ultrapure DI water (NANOpure Diamond System, Barnstead International, Dubuque, IA).

A balanced salt solution (BSS) was used for islet experiments which contained 125 mM NaCl, 5.9 mM KCl, 1.2 mM MgCl₂, 2.4 mM CaCl₂, 25 mM tricine, and brought to pH 7.4 before addition of 0.1% BSA (Bovine serum albumin). Different glucose concentrations were added as described in the text, and the BSS was filtered with a 0.2 μm nylon syringe filter (Pall Corporation, Port Washington, NY) prior to delivery to the microfluidic system.

Islets of Langerhans

Human islets were purchased from Prodo Laboratories Inc. (Aliso Viejo, CA) from donors who had not been diagnosed with diabetes. Human islet samples (85–95% pure) were incubated for a minimum of 1 day in complete Prodo Islet Media Standard PIM(S) at 37C and 5% CO₂ upon delivery.¹⁸ Human islet samples were obtained from deidentified cadaveric organ donors and, therefore, were exempt from Institutional Review Board approval. Donor characteristics are provided in **Table 2-1**.

Table 2-1. Donor characteristics for human islets.

	Donor 1	Donor 2	Donor 3	Donor 4	Donor 5
Sex	F	M	F	M	F
Age	60	48	39	56	42
Height (inches)	61	73	63	69	65
Weight (lbs)	139	157	124	222	141
BMI	25.8	20.2	22.1	32.8	23.5
HbA1c (%)	5.1	5.2	5.6	5.3	5.4

Microfluidic Device

The microfluidic device was fabricated using methods described previously.⁸ Briefly, conventional soft lithography was used to make a 400 x 200 μm (width x depth) channel in PDMS. The access holes at the ends of the channel were made using a 0.508 mm diameter titanium nitride hole punch (SYNEO, Angleton, TX). A hole for loading islets was made in the middle of the channel length using a 400 μm diameter punch (Welltech, Taichung, Taiwan). The PDMS was irreversibly bonded to a 25 x 75 x 1 mm (width x length x thickness) glass coverslip (VWR, Randor PA) after plasma oxidation of both pieces. The glass coverslip formed the bottom of the channels.

To maintain the temperature of the islet chamber at 37 °C, a thermofoil heater (Omega Engineering, Inc., Stamford, CT) was placed underneath the microfluidic device and a thermocouple sensor was applied adjacent to the islet chamber on top. A controller (Omega Engineering) was used to maintain the temperature at 36.5 +/- 0.5 °C. To perform perfusion, the

outlet from two syringe pumps were connected via a junction to the inlet access hole of the device. The total flow rate into the microfluidic device was maintained at 5 mL min⁻¹. Perfusate was collected via a 10 cm length of 0.508 µm i.d. Tygon tubing connected to the outlet. Fractions were collected from this tube every 2 min into a new 200 mL Eppendorf tube.

To load islets, the device was filled with BSS containing 20 mM glucose and a number of islets were introduced into the islet loading port with the exact number given in the text and figure captions. The islet loading port was then covered with PCR tape and the input and output tubing were removed. The device was placed in a 37 °C, 5% CO₂ incubator for 10 min to allow islets to settle to the bottom and attach to the glass surface. At the end of the 10 min, the device was removed from the incubator, the tubing reattached, and flow initiated with BSS containing 20 mM glucose. The islets were allowed to equilibrate to the flow for 15 min prior to fractions being collected. The glucose level delivered to the islets was varied by adjusting the syringe pump flow rates as described in the text. At the end of the experiment, all fractions were centrifuged to remove air bubbles, pipetted into a 96-well plate, and assayed as described below.

Islets were removed from the device and lysed to measure the total glucagon content as described.⁶⁷ All islets were removed from the device by aspiration and placed into a 200 µL tube. The tube was centrifuged, and a 10 µL pipette was used to transfer all islets to a new tube. A 90 µL volume of acid-ethanol mixture (750 mL of 95% ethanol; 15 mL of 5 M HCl; 235 mL of H₂O) was added and the tube sonicated for 5 min.⁶⁸ The lysate was kept at -20 °C prior to analysis if not read immediately. For analysis, 10 µL of the lysate solution was diluted to 200 µL with BSS. To ensure the concentration of the lysate was within the calibration curve, three dilutions were then performed: 10 µL of the 200 µL lysate solution was diluted to 100 µL with BSS; 10 µL of this newly made solution was diluted to 100 µL using BSS; 10 µL of this solution was then removed and diluted to 100 µL with BSS. 10 µL of each of these three solutions was added to the 96-well plate, along with the perfusion fractions, and assayed using TR-FRET.

TR-FRET Glucagon Assay

In addition to the fractions collected from the perfusion and the lysate, each 96-well plate (HTRF 96-well low volume white plate) had three replicates of 2000, 1000, 500, 250, 125, 62.5, 31.25, 15.6 and 0 pg mL⁻¹ standard glucagon solutions made in BSS. Reagents from the TR-FRET glucagon assay kit (10 mL) were pipetted into each well using a multi-channel pipette. The well

plate was covered with film and incubated 12–14 h at room temperature in the dark. A plate reader (SpectraMax iD5, Madison, WI) was used to measure the TR-FRET according to the manufacturer's protocol. Briefly, excitation light (360 nm) was on for 50 μ s, followed by a 100 μ s delay, and a 600 μ s recording time of the two FRET channels (620 and 665 nm). This timing protocol was repeated every 2 ms for 100 cycles.

The average FRET signal from the 0 pg mL^{-1} standard solution was subtracted from all FRET measurements. FRET ratios are presented as the ratio of the emission at 665 nm to that at 620 nm multiplied by 10,000. Calibration curves were generated by averaging the FRET ratio from the three replicates of each standard glucagon solution and plotting these values vs. the concentration of glucagon.

Finite Element Analysis

The proposed microfluidic system featuring islets was developed in a finite element simulation software (COMSOL Multiphysics v4.3, COMSOL Inc., Stockholm, Sweden). Flow rates were solved using the incompressible Navier–Stokes equation with a no slip boundary condition on solid surfaces; islets were modeled as porous spheres. All simulation parameters are given in **Table 2-2**.

Table 2-2. Model parameters for the finite element simulation.

Parameters of the finite element simulation	
Temperature (T)	310.15 K
Viscosity (η)	$1 \times 10^{-3} \text{ N s m}^{-2}$
Density (ρ)	$1 \times 10^3 \text{ kg m}^{-3}$
Volumetric Flow Rate (V)	$5 \mu\text{L min}^{-1}$

Data Analysis

To quantify glucagon, the FRET ratio from each fraction was converted to glucagon concentration (pg mL^{-1}) using the calibration from the same plate with the amount of glucagon (pg) then determined. The lysate dilution which fell within the calibration curve was used to determine the amount of glucagon (pg) in the total lysate by accounting for the various dilutions.

Secretion traces are presented as percent glucagon released, which was determined by calculating the percent of glucagon in each fraction with respect to the total glucagon (the sum of the lysate and all fractions).⁶⁷The number of islets used in each experiment are provided in the text or figure caption, but the islet equivalents were not calculated.

Results

The measurement of glucagon secreted from pancreatic islets of Langerhans is typically carried out with macro-perfusion systems and offline ELISAs. Development of microfluidic systems to hold islets and deliver stimulants would provide an additional level of control and automation. Homogeneous assays for measurement of glucagon would decrease analysis times by reducing the number of steps for detection. Here, we have coupled a straightforward PDMS microfluidic device for islet perfusion with fraction collection and subsequent glucagon quantification with a TR-FRET homogeneous assay. We anticipate the simplicity of the system will enable other researchers to use similar methods to perform more complex experiments.

Glucagon Assay

A commercially available TR-FRET assay was used for quantitation of glucagon. In this system, a “sandwich assay” is used with different fluorophores attached to antibodies recognizing different epitopes. One of the antibodies was labeled with a lumi4-terbium cryptate donor ($\lambda_{\text{ex}} = 340 \text{ nm}$, $\lambda_{\text{em}} = 620 \text{ nm}$), and the other was labeled with a d2 red acceptor ($\lambda_{\text{ex}} = 620 \text{ nm}$, $\lambda_{\text{em}} = 665 \text{ nm}$). FRET between the two fluorophores confirmed the presence of the hormone and the ratio of intensities from 665 and 620 nm allowed for accurate quantitation. An advantage of this assay is the long-lived fluorescence lifetime of the donor (1–2 ms), which allowed for the two emission channels to be measured 100 μs after the excitation light was turned off, enabling low background measurements.

Standard glucagon solutions were subjected to measurement with this system and resultant calibration curves of FRET ratio versus glucagon concentration showed a reproducible linear response (**Figure 2-1**). The relative standard deviations of the points ranged from 1 to 12%, and the calculated limit of detection (LOD) was 15 pg mL^{-1} . These results demonstrated good reproducibility and a sensitivity compatible with concentrations of glucagon typically released from islets.^{10,61} These values are similar to those reported for commercial ELISA systems, but

without the necessity for wash steps, although an overnight (12 - 14 h) incubation period was required for producing high quality calibration curves in our hands. Shorter incubation times were attempted but resulted in higher RSD and/or lower linearity. Nevertheless, the LOD was sufficient to proceed with the development of the microfluidic system.

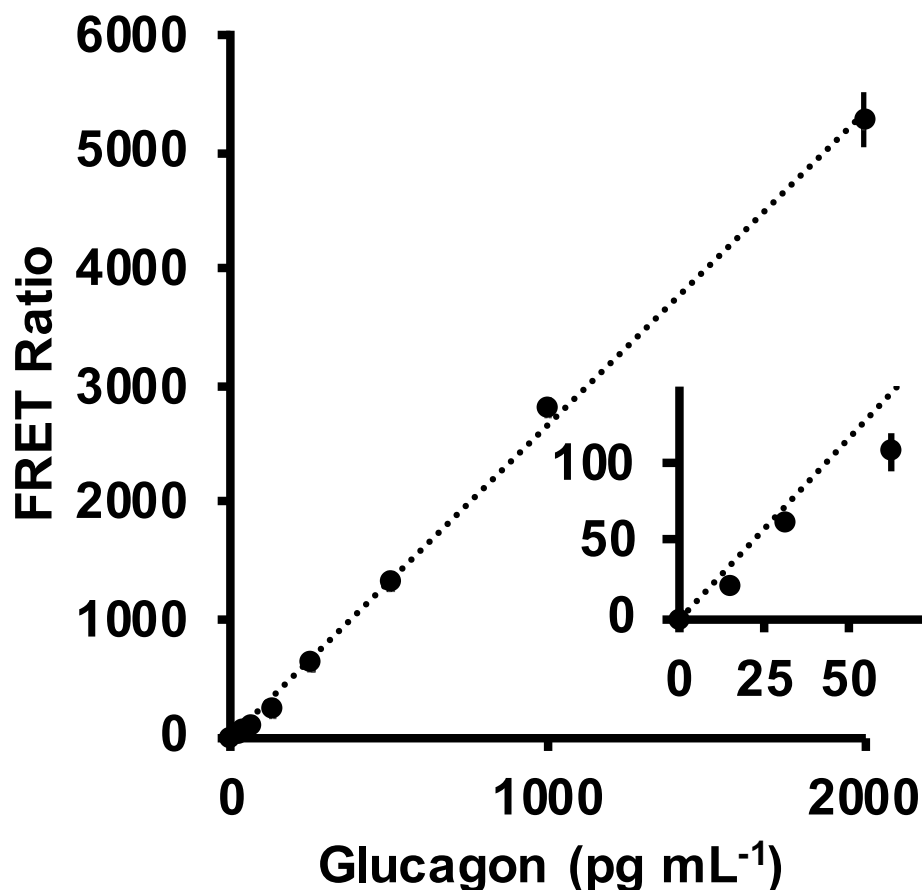


Figure 2-1. Calibration of TR-FRET assay. A representative calibration of the TR-FRET assay is shown. The points are the average of 3 replicates and the error bars are ± 1 standard deviation. The inset shows the lower region of the curve. The plot was fit with a linear regression line $y=2.6659x$ ($r^2 = 0.999$).

Microfluidic System

Once the glucagon assay was confirmed to produce LOD sufficient for islet measurements, a microfluidic device was designed to hold islets, perfuse glucose, and allow for fraction collection. The goals of the device were to have simple construction and operation, yet still provide a rapid response from islets housed in the device. Additionally, the tissue needed to be easy to load and recover from the device. These goals were achieved using a PDMS/glass microfluidic device that

contained a single flow channel with a central loading port to add and remove islets (**Figure 2-2A**). After adding islets, the loading port was sealed with PCR tape to keep solution within the device.

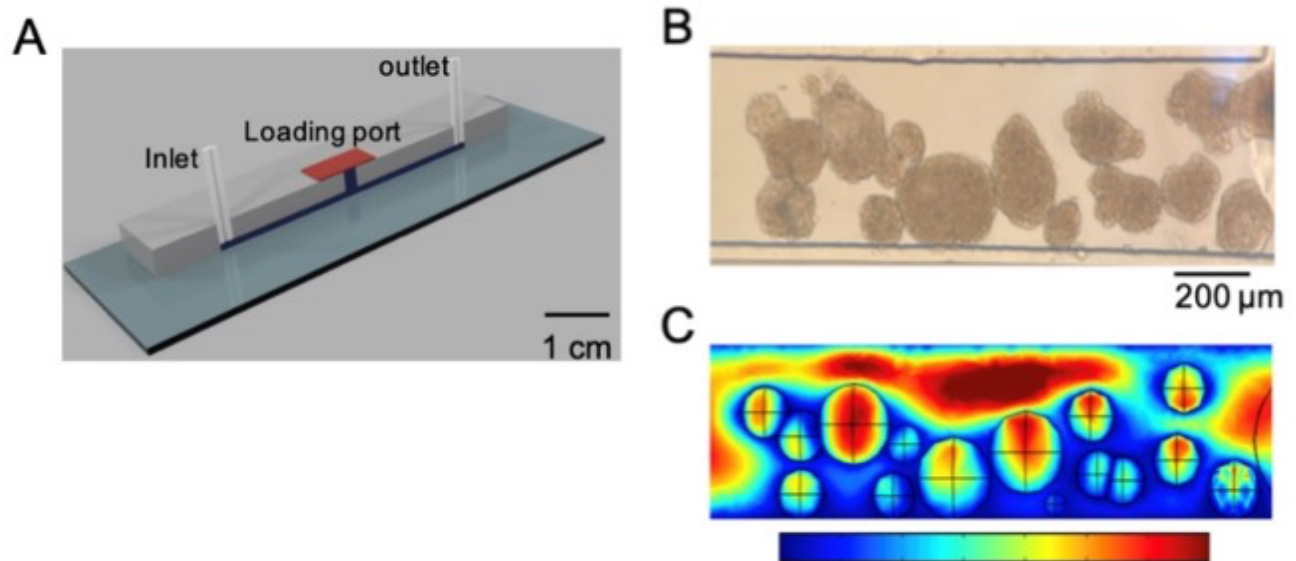


Figure 2-2. Microfluidic system. (A) A 3D drawing of the PDMS/glass microfluidic device used in this report. The outputs of two syringe pumps were coupled at a tee (not shown) and input into the inlet port of the device. Islets were loaded through the central loading port and covered with a piece of PCR film. Tubing at the outlet (not shown) was used to collect fractions of the perfusate every 2 min. (B) An image of the microfluidic device loaded with human islets was used to mimic the placement and size distribution in a finite element model. (C) The picture in (B) was used to build a finite element model of fluid flow in the device. The image is from the simulation and shows a composite view from a slice of the fluid velocity taken in the middle of the channel and a surface plot of the shear stress on the islets. The scale bar at the bottom of the image is for both the fluid velocity and shear stress. The range for shear stress is 0.0–75 mPa, and the range for velocity is 0.0– 1.25 mm s⁻¹.

To perform perfusion, the output from two syringes driven by syringe pumps were connected with a T-junction and then to the inlet port on the microfluidic device. The tubing was inserted into the hole punched in the PDMS, creating an interface that did not require sealant or glue. The ratio of the flow rates from the two syringe pumps was then varied to adjust the concentration of stimulant into the device while the total flow rate was maintained at a constant 5 mL min⁻¹.

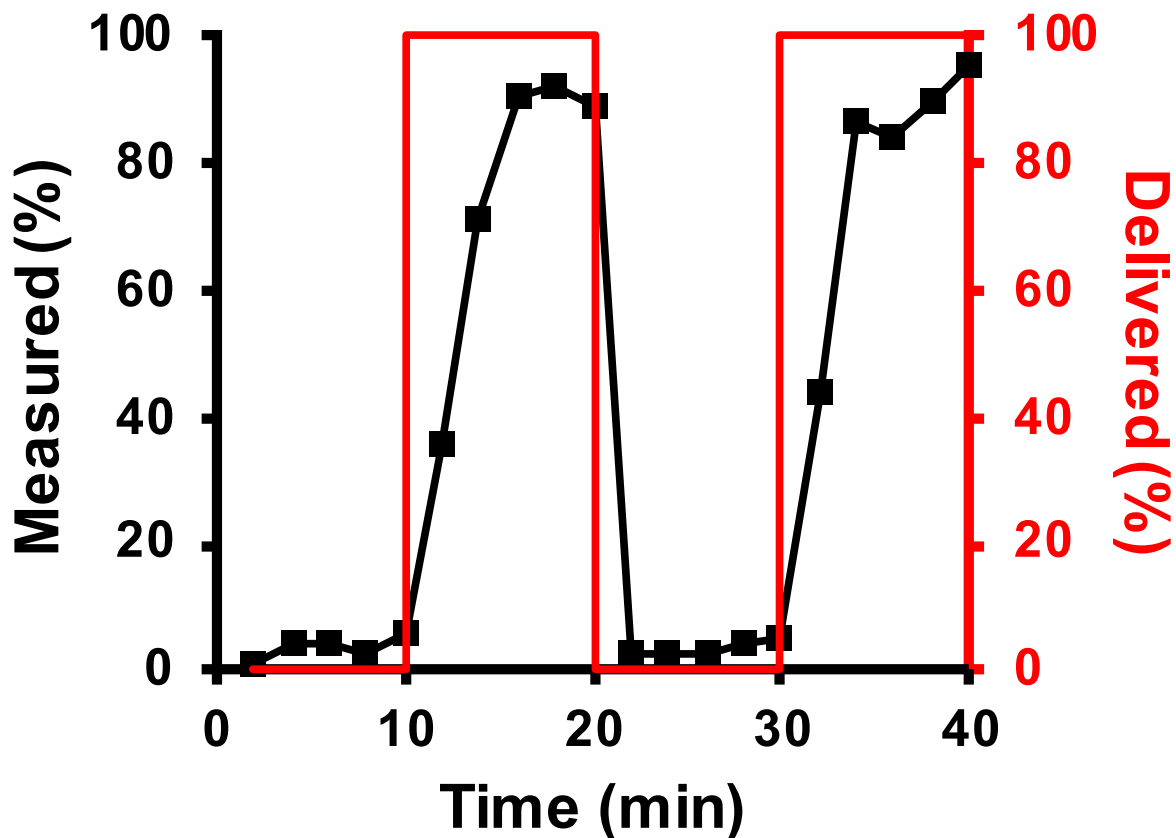


Figure 2-3. Flow dynamics. Low (0 pg mL^{-1}) and high (1200 pg mL^{-1}) glucagon concentrations were delivered to the device through the syringe pumps in a pattern shown by the red line (corresponding to the right y-axis). The flow through the device was fractionated every 2 min and measured using the TR-FRET assay. The amount of glucagon in each fraction is shown by the data points and corresponds to the left y-axis.

To ensure that the experimental conditions would not be detrimental to the islets, a 3-dimensional finite element simulation was used to model the fluid flow. To mimic experimental conditions as closely as possible, 15 islets were placed in a device and a photograph was obtained (Figure 2-2B) to guide the sizes and locations of islets in the simulation. The islets ranged from $100 - 250 \text{ }\mu\text{m}$ in diameter and they were modeled as porous spheres with a porosity of 0.1 and permeability of 10^{15} m^2 . The flow rate into the device was $5 \text{ }\mu\text{L min}^{-1}$ and other model parameters are provided in **Table 2-2**. The linear fluid velocity (mm s^{-1}) through the device is shown in Figure 2-1C and indicated that the islets influenced the flow of the liquid in the channel. To determine how the flow conditions may affect the islets, the shear stress on the islet surfaces were calculated. In Figure 2-2C, the islet surfaces have the shear stress overlaid and indicated a maximum of 71 mPa on the largest islet in the simulation, slightly below the physiological shear stress range.⁶⁹

These results indicated that the design would not produce damagingly high levels of shear to the islets.

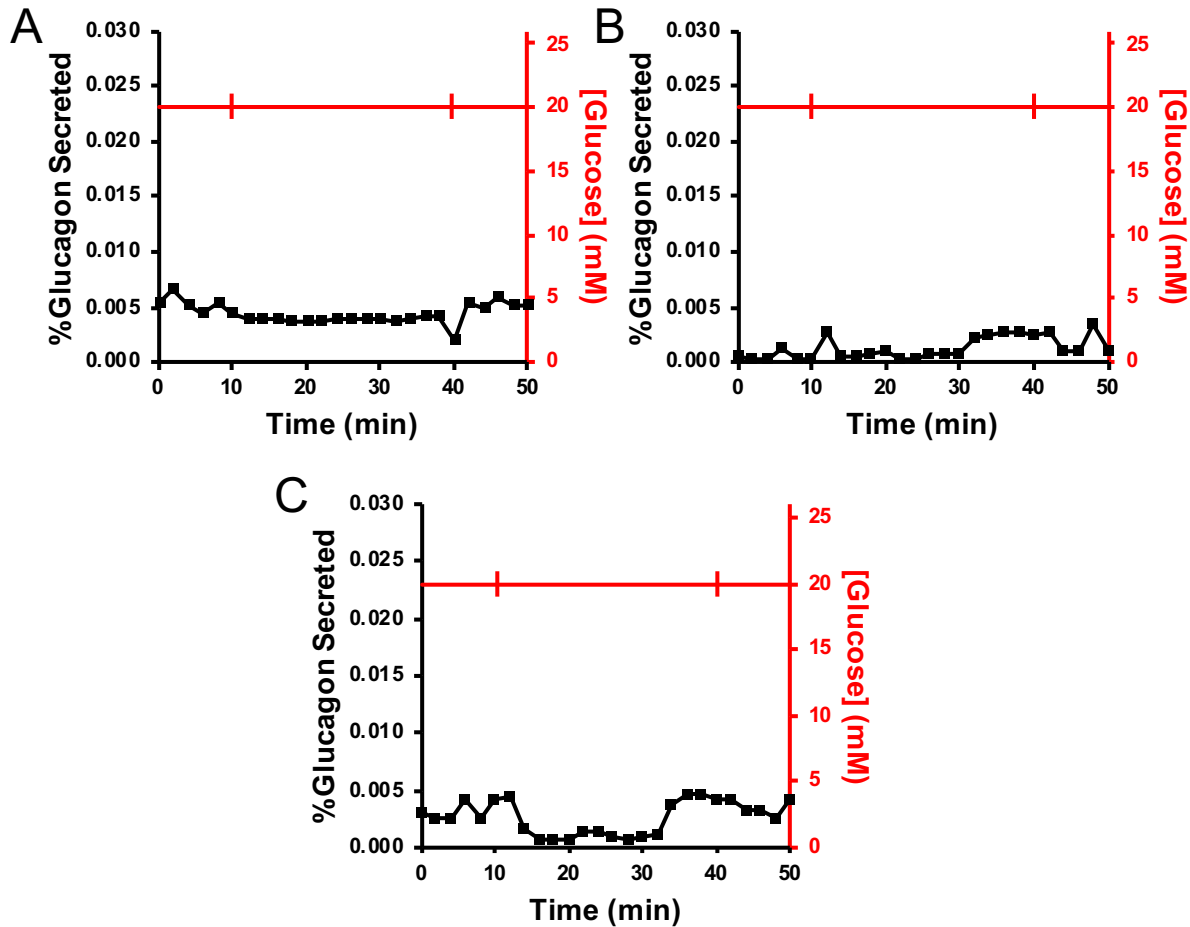


Figure 2-4. Control experiments. 25 islets from Donor 5 were exposed to a constant 20 mM glucose for the duration of the experiment. At 10 and 40 min, the flow rates from the two syringe pumps were switched to mimic the experiment for initiating glucagon release (for example, the experiment shown in Figure 2-3).

Upon finalization of the simulation, the dynamic response of the microfluidic system was determined by perfusing step changes of glucagon through the device. To perform the perfusion, syringe 1 was filled with 3 mL of BSS and syringe 2 was filled with 3 mL BSS buffer containing 1200 pg mL^{-1} glucagon. The device was flushed with syringe 1 for 15 min prior to the start of the experiments to condition the device. For the next 40 min, flow from syringe 1 and syringe 2 was alternated for 10 min each. **Figure 2-3** shows these results with the glucagon delivery profile shown as the red line, and the glucagon measured as the black points. Based on the volumes of the inlet and outlet tubing and the channel, the time required for glucagon to travel from the T-junction

into the fraction collection tubes was 5.25 min. This time was subtracted from the glucagon delivery profile (red line in Figure 2-3) and demonstrates that the glucagon measured in the fractions mirrored the delivery profile upon this correction. The average response time, defined as the time required to increase or decrease the signal from 10% to 90% of the final signal was 2 fractions or 4 min. Additionally, we did not observe a significant difference in the TR-FRET signal during subsequent perfusions of either glucagon (10–20 min vs. 30–50 min) or BSS (from 0–10 min vs. 20–30 min), which indicates that any non-specific adsorption in the device was undetectable.

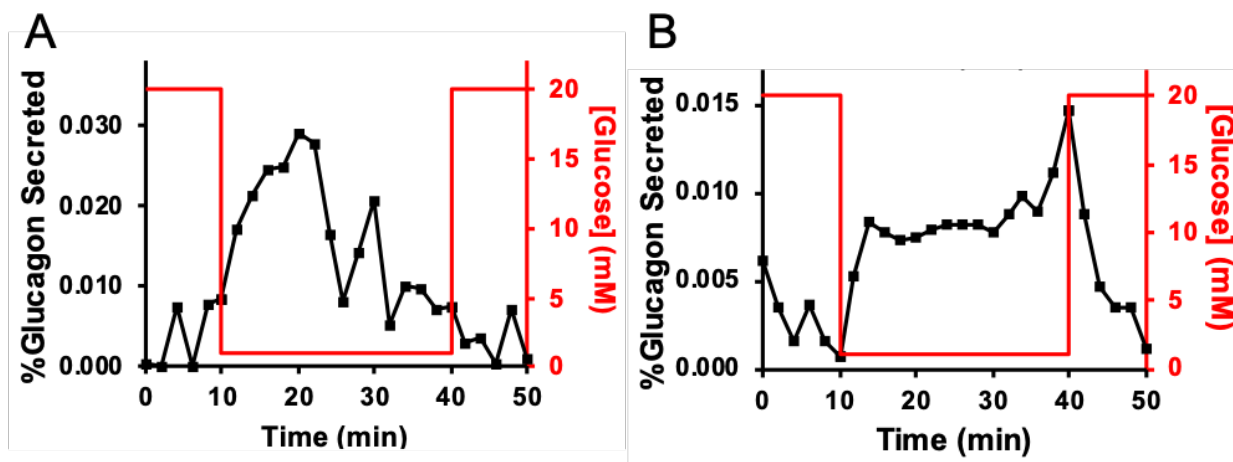


Figure 2-5. Representative glucagon secretion profiles. In both traces, the measured glucagon levels are shown by the black points and correspond to the left y-axis, while the glucose profile delivered to the device is shown as a red line and corresponds to the right y-axis. (A) A representative trace from a group of 30 islets from donor 4 that released in a “burst” pattern. (B) A representative group of 45 islets from donor 4 that released glucagon in a “sustained” pattern.

Glucagon Measurements

Following method development of the system with standard glucagon solutions, a batch of human islets were loaded into the device. Initial experiments were performed to ensure islets would not respond to variations from changing the syringe pump flow rates. To perform these control experiments, both perfusion syringes were filled with BSS containing 20mM glucose. The first syringe pump delivered solution to the device for 10 min, after which the flow was switched to the second syringe pump for the next 20 min. After this time, the flow was switched back to the first syringe for the last 20 min. As shown in **Figure 2-4**, the islets did not respond to these changes in the solutions with a significant change in the glucagon secreted. This protocol was repeated a total of 3 times, each replicate with different islets.

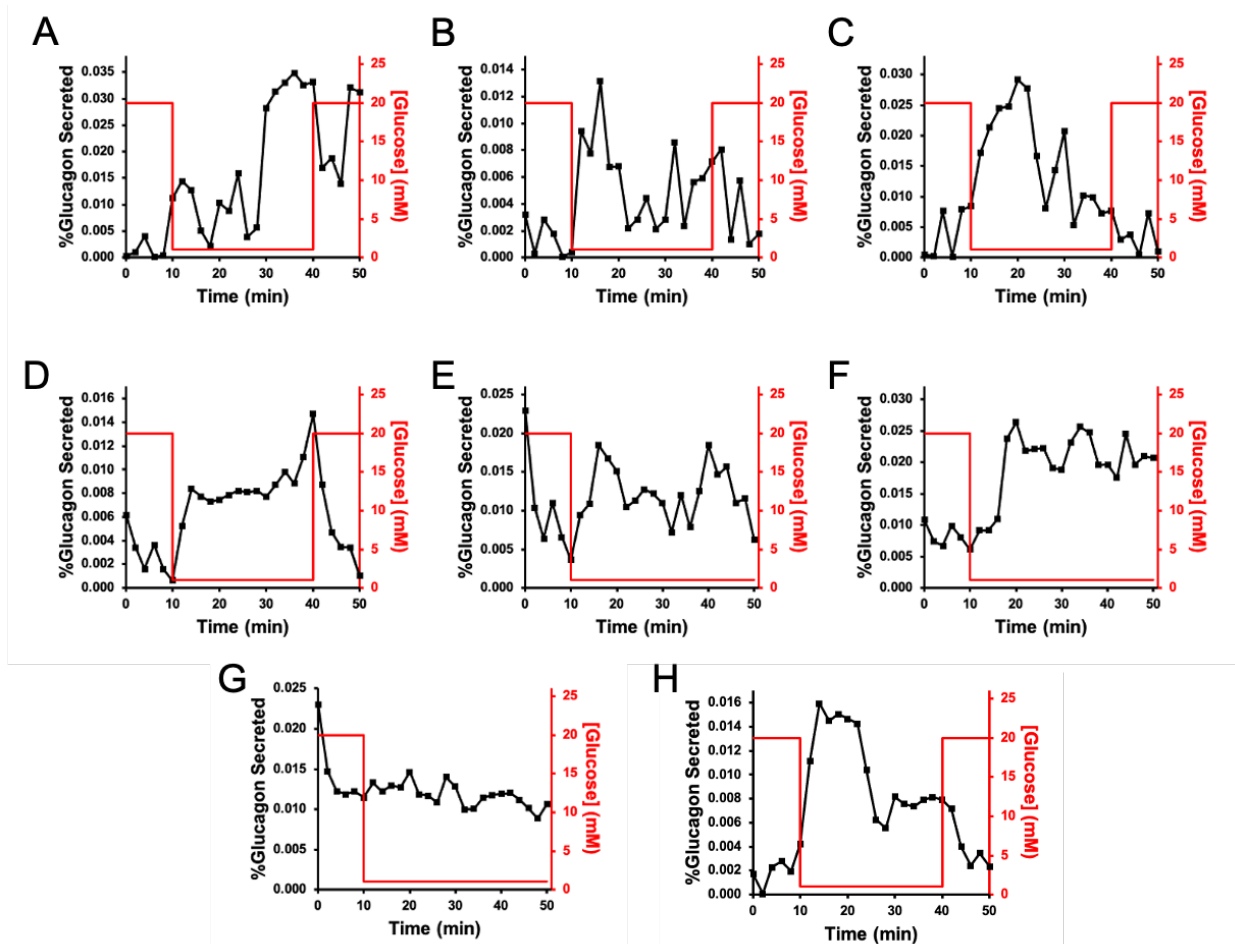


Figure 2-6. All glucagon secretion profiles are shown where the total glucagon content from the islets were assayed after the experiment. The number of islets and donor for each panel were: **A)** 30 islets, donor 4 (burst), **B)** 20 islets, donor 4 (burst); **C)** 30 islets, donor 4 (burst); **D)** 45 islets, donor 4 (sustained); **E)** 30 islets, donor 3 (burst); **F)** 25 islets, donor 3 (sustained); **G)** 28 islets, donor 3 (no response); **H)** 25 islets, donor 5 (burst).

Upon confirming that the switch in perfusion flows did not induce changes in glucagon release, we then tested the ability to measure glucagon secretion in response to glucose changes. To perform these experiments, islets were placed in the microfluidic device, allowed to adhere for 10 min, and perfused with 20 mM glucose in BSS. After this period of basal release (usually 10 - 15 min), the glucose level was decreased to 1 mM. For some experiments, the glucose concentration was held at 1 mM for the remainder of the experiment ($n = 3$); in other experiments, the glucose concentration was increased back to 20 mM ($n = 4$). Due to the high variability in islet composition, secretion amounts were normalized to the total glucagon content in the islet population as described in the Materials and methods. The glucose time curve was also adjusted by 5.25 min to account for the volume of the device and tubing.

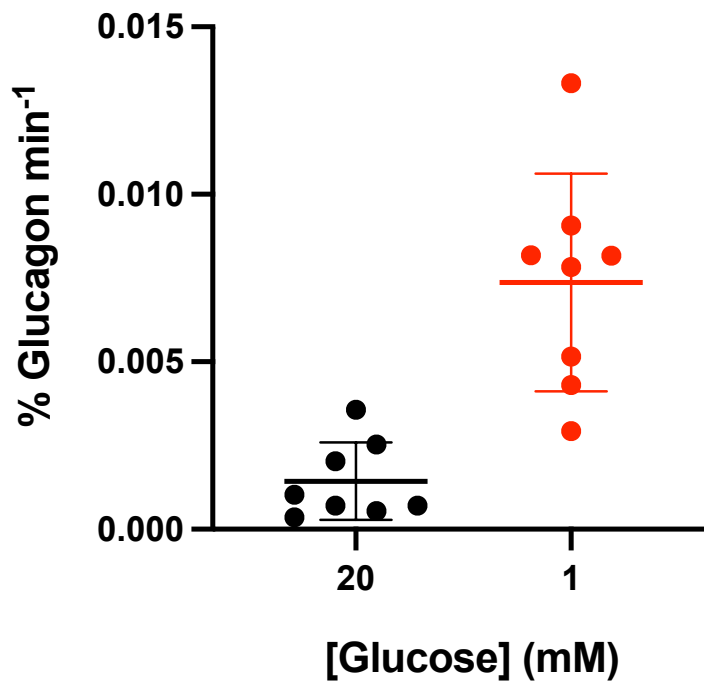


Figure 2-7. Average glucagon levels. The total glucagon secretion levels normalized over the collection time (total glucagon min⁻¹) for all traces shown in Figure 2-6 were averaged and shown as a function of glucose level. The difference in the amount of glucagon released during 1 mM glucose was significantly higher than that at 20 mM glucose ($p = 0.002$, 1-tailed Student's t-test). Average is shown as the thick horizontal line with error bars equal to ± 1 standard deviation.

Qualitatively, most experiments exhibited one of two patterns of release, either a burst of glucagon secretion followed by a decline in the rate of release, or they showed a sustained level of release during the entire stimulation. **Figure 2-5** shows a representative trace from each of these groups. Figure 2-5A illustrates a “burst” pattern of glucagon released (black points) in response to different glucose concentrations (red). These results were from a batch of 30 islets from donor 4. This “burst” pattern was observed for five experiments: one experiment from islets from donor 3, three experiments with islets from donor 4, and one experiment from donor 5. Figure 2-5B shows a “sustained” pattern of glucagon release from a batch of 45 islets from donor 4. This pattern was observed for two of the experiments, with one each from donor 3 and 4. In one experiment (with a batch of islets from donor 3), a change in glucagon release was not observed. **Figure 2-6** shows all perfusion responses from each set of islets tested. At this time, it is unknown why some experiments showed one secretion profile versus another, although a previous report shows similar “burst” profiles with 10 islets.¹⁰

The percent glucagon release during stimulation with high and low glucose was quantified for all experiments ($n = 8$) and normalized to the stimulation period. The results are shown in the scatter plot in **Figure 2-7** with the average shown as the horizontal bar and the error bars corresponding to ± 1 SD. The average (SD) percent glucagon release during stimulation with 1 mM glucose was $7\text{-fold higher at } 0.007 \pm 0.003\% \text{ min}^{-1}$ compared to that measured at 20 mM glucose, $0.001 \pm 0.001\% \text{ min}^{-1}$. A 1-tailed Student's t-test indicated that these results were significantly different ($p = 0.002$) for the two glucose conditions tested.

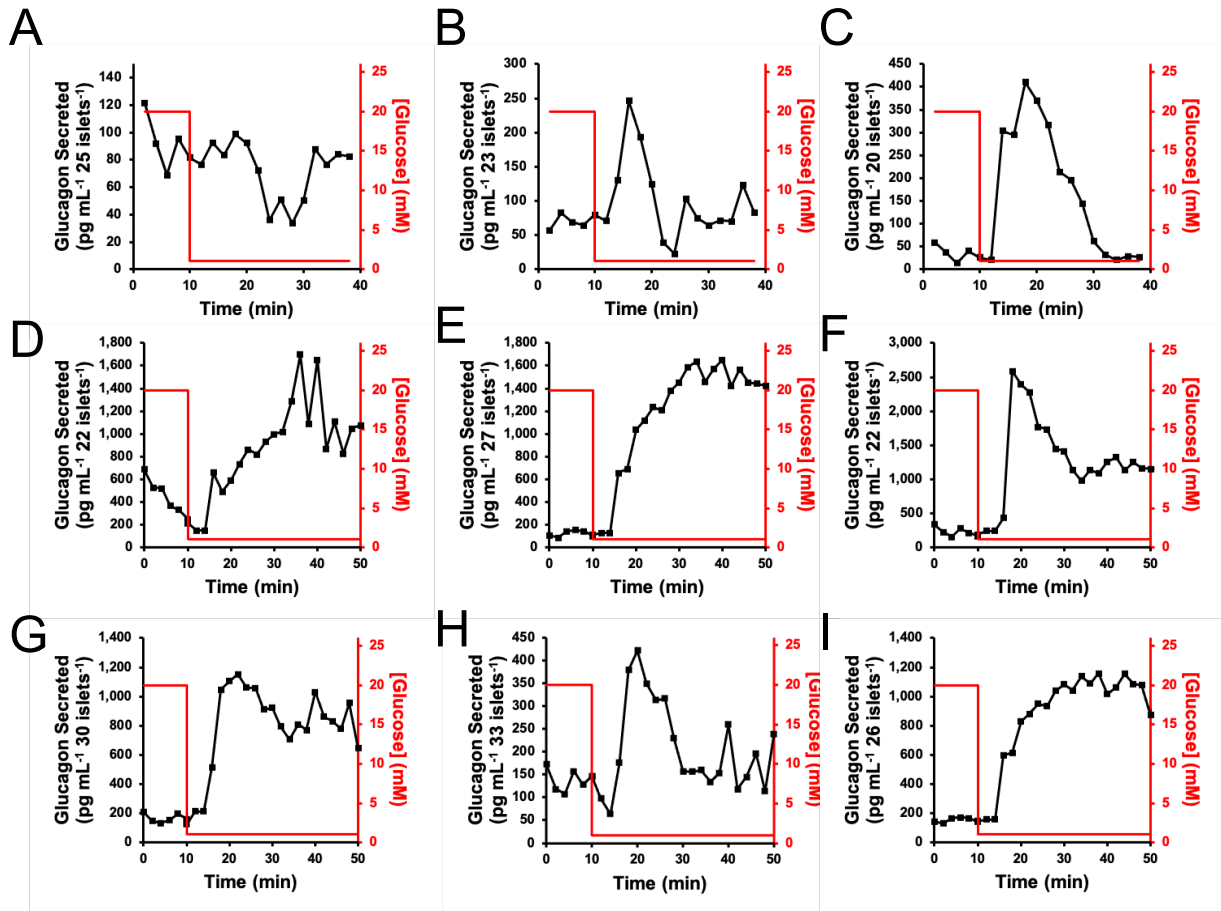


Figure 2-8. Additional glucagon secretion profiles. Shown are additional experiments that were performed on batches of islets, but the islets were not collected after the experiment. These are provided to show more of the profiles but were not included in the data shown in Figure 2-5. (A-C) donor 1; (D-E) donor 2. The secretion values were not normalized to the islet number, and the islet number is given in the y-axis.

Finally, in some initial experiments, the islet glucagon content after the experiment was not measured because the method was being developed. In these experiments, calculation of the percent glucagon released was not performed, but the traces are shown in **Figure 2-8**. Because the

total glucagon content was not measured, these traces were omitted from statistical analysis and are shown here to demonstrate that other experiments from different donors also showed the secretion profiles mentioned above. Three experiments exhibited a “burst” profile, four showed the “sustained” release, and two did not show much release upon stimulation with low glucose.

Conclusions

Information regarding glucagon release from human islets of Langerhans is much less comprehensive relative to that for insulin secretion. The combination of a simple and robust microfluidic system with a TR-FRET assay described here is expected to provide a relatively simple glucagon measurement method while still providing valuable information regarding the release of this peptide hormone. For example, it could be used to further examine “burst” versus “sustained” secretion profiles. With the LOD of this assay, we approximate that release from about 5 islets could be measured, which may allow the dynamics of release to be observed more clearly. Finally, the dimensions of the microfluidic device are amenable to fabrication by other means, including milling or hot embossing in other materials, which could enable simple and rapid high throughput production while a mechanical system could be used to automate the fraction collection process. Because the TR-FRET assay can be performed without washing steps, the sensitivity and simplicity of the system are ideal for those investigating the release of glucagon.

CHAPTER 3

AN AUTOMATED SYSTEM FOR LOW VOLUME MEASUREMENT OF GLUCAGON AND INSULIN FROM HUMAN PANCREATIC ISLETS OF LANGERHANS

Introduction

Monitoring of cellular secretions is principal to the investigation of biological systems and cellular communication. Resolved secretion profiles provide insight into the mechanisms of a cell in response to an environmental stimulus.^{18,36,70,71} Specifically, for blood glucose regulation, secretion profiles for insulin and glucagon are of interest.^{29,30,36} Furthermore, disruptions to cellular secretion patterns can signal cellular stress and failures of biological pathways.^{17,72,73} For example, disrupted insulin and glucagon secretions are hallmarks of diabetes.^{8,36} To better characterize these release profiles, development of analytical systems that can detect and quantify trace amounts of peptides secreted from cells is required.^{10,25,44,66,74} Additionally, temporal resolution is needed to understand how hormone concentrations change as a function of time, because characterization of their pulsatile behavior is important, and the periods of oscillation are short.^{8,44,75,76}

The study of insulin release dynamics from islets of Langerhans has been extensively studied through the advancement of analytical techniques focused toward the rapid measurement of insulin using microfluidics.^{25,77} As previously mentioned, insulin is a hormone released from islets of Langerhans that lowers blood glucose levels in vivo following intake of glucose from a meal.⁷⁸ Many studies have focused on the measurement of insulin from small batches of pancreatic islets; however, few have studied the release of glucagon, which raises blood sugar during periods of fasting (opposite of insulin). Furthermore, the pulsatile release of these two hormones are 180 degrees out of phase with each other. Despite this highly coordinated relationship of insulin and glucagon, previous work has focused on independent measurement of the two peptides while simultaneous measurement has not been extensively studied.

In Chapter 2, we demonstrated the use of a FRET-based assay for time-resolved measurement of glucagon concentrations released from human pancreatic islets. To probe the relationship between insulin and glucagon release dynamics, we have combined the FRET-based assay for glucagon quantitation (Chapter 2) with a second TR-FRET assay specific for insulin. Additionally, this system introduces an improved fraction collection system, which is enabled by

a computer numerical control (CNC) machine for automated collection of fractions onto a low volume well plate. This highly-automated and improved fluid flow system could be implemented into other systems used for hormone quantitation measurements.

The simultaneous measurement of insulin and glucagon released from pancreatic islets will enable a deeper understanding regarding the secretion dynamics of these hormones and their interconnected relationship. This information will lead to a better understanding of type II diabetes and enhanced development of therapeutics.

Methods and Materials

Chemicals and Reagents

Dextrose was obtained from Fisher Scientific (Pittsburgh, PA). The TR-FRET glucagon assay was obtained from Cisbio (Waltham, MA). All other reagents were purchased from Sigma-Aldrich (St. Louis, MO) unless noted otherwise. All solutions were made with ultrapure DI water (NANOpure Diamond System, Barnstead International, Dubuque, IA).

A balanced salt solution (BSS) was used for islet experiments which contained 125 mM NaCl, 5.9 mM KCl, 1.2 mM MgCl₂, 2.4 mM CaCl₂, 25 mM tricine, and brought to pH 7.4 before addition of 0.1% BSA. Different glucose concentrations were added as described in the text, and the BSS was filtered with a 0.2 μm nylon syringe filter (Pall Corporation, Port Washington, NY) prior to delivery to the microfluidic system.

Islets of Langerhans

Human islets were purchased from Prodo Laboratories Inc. (Aliso Viejo, CA) from donors who had not been diagnosed with diabetes. Human islet samples (85–95% pure) were incubated for a minimum of 1 day in complete Prodo Islet Media Standard PIM(S) at 37 °C and 5% CO₂ upon delivery. Human islet samples were obtained from deidentified cadaveric organ donors and, therefore, were exempt from Institutional Review Board approval. Donor characteristics are provided in Table.

Table 3-1. Donor characteristics for human islets.

	Gender	Age	Height (inches)	weight (lbs)	BMI	HbA1c (%)	date
Donor 1	F	62	58	123	25.8	5.7	9/27/21
Donor 2	M	39	71	208	29	5.4	10/5/21

Microfluidic Device Fabrication

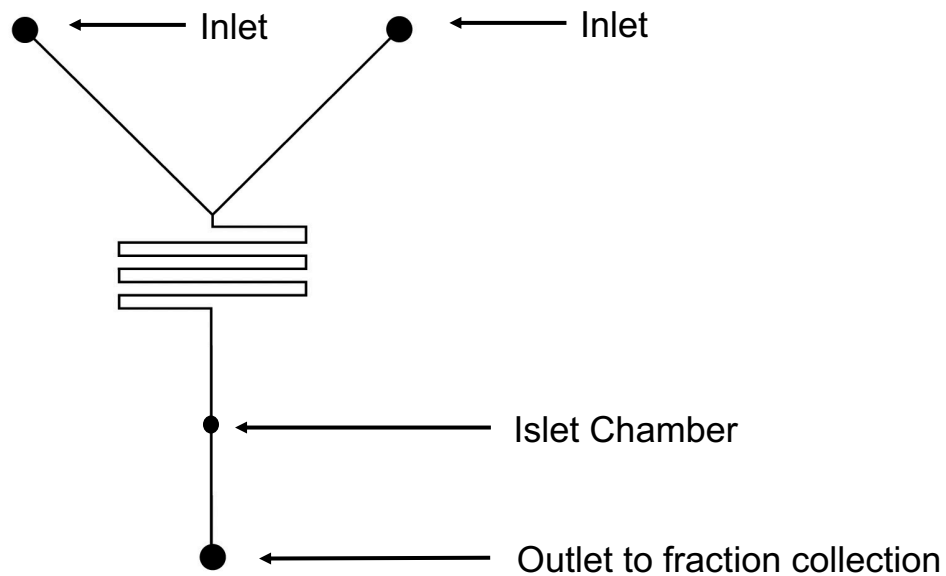


Figure 3-1. Microfluidic device design. A 2D display of the microfluidic device design, includes two inlets to allow for a dual perfusion of buffers to the islets chamber, where the islets are loaded and remain during an experiment. The mixing junction joins the fluid streams from the two inlets, and the serpentine channel design after the mixing cross allow for the fluid stream to be homogenized prior to the islet chamber. The outlet directs fluid flow to the fraction collection system.

The microfluidic device shown in **Figure 3-1** was fabricated using methods described previously. Photolithography and wet etching techniques were used to make 100 x 50 μm (width x depth) channels in glass.¹² The access holes at the ends of the channel were made by irreversibly bonding cubes of PDMS to the top surface of the glass device after plasma oxidation of parts. Following the binding of PDMS to the glass surface, a 0.508 mm diameter titanium nitride hole

punch (SYNEO, Angleton, TX) was used to puncture the PDMS from the top of the cubes to the endpoints of the channel.

Microfluidic Experiments with Human Islets

To maintain the temperature of the islet chamber at 37 °C, a thermofoil heater (Omega Engineering, Inc., Stamford, CT) was placed underneath the microfluidic device and a thermocouple sensor was applied adjacent to the islet chamber on top. A controller (Omega Engineering) was used to maintain the temperature at 36.5 ± 0.5 °C. To perform perfusion, a variable pressure system (Elveflow) was established to control dynamic fluid flow to device.⁷⁹ Fluid reservoirs containing BSS with differing concentrations of glucose were pressurized with compressed air from a piezoelectric pressure regulator.⁷⁹ Between the pressurized fluid reservoir and the microfluidic device, an inline flow monitor connected to the pressure regulator continuously monitored flow rates and provided feedback to ensure stable flow rates to the device. The total flow rate delivered to the device was set to $5 \mu\text{L min}^{-1}$, which was equal to the sum of the flow rates of inlet 1 and inlet 2.

Fraction Collection with CNC Machine

The outlet of the microfluidic device was connected to a 150 μm diameter capillary, which was attached to the head of the CNC machine. The CNC platform had a custom 3-D printed 96-well plate holder screwed to the moveable platform. The end of the capillary was zeroed 15 mm above the bottom of the first well of the 96-well plate. The program code controlling the machine directed one action at a time. First, the capillary was lowered 15 mm to the bottom of the first well. A 178 s pause allowed sample deposition into the well. Next, the CNC machine made a series of three moves to reach the next well: raised 15 mm from the bottom of the well, moved laterally 9 mm over the next well, and finally lowered the capillary 15 mm into the adjacent well, where sample was deposited for 178 s. The travel time between wells was 2 s and the pause time was 178 s; thus, total time spent per well was 180 s. This enabled three-minute fraction collection for all experiments and 15 μL of sample to be collected per well.

To load islets, the device was filled with BSS containing 20 mM glucose and 30 islets were introduced into the islet loading port with the exact number given in the text and figure captions. The islet loading port was then covered with PCR tape and input and output tubing were

removed.^{68,75} The device was placed in a 37 °C, 5% CO₂ incubator for 10 min to allow islets to settle to the bottom and attach to the glass surface. At the end of the 10 min, the device was removed from the incubator, the tubing was reattached, and flow was initiated with BSS containing the desired concentration of glucose. The islets were allowed to equilibrate to the flow for 15 min prior to fractions being collected.

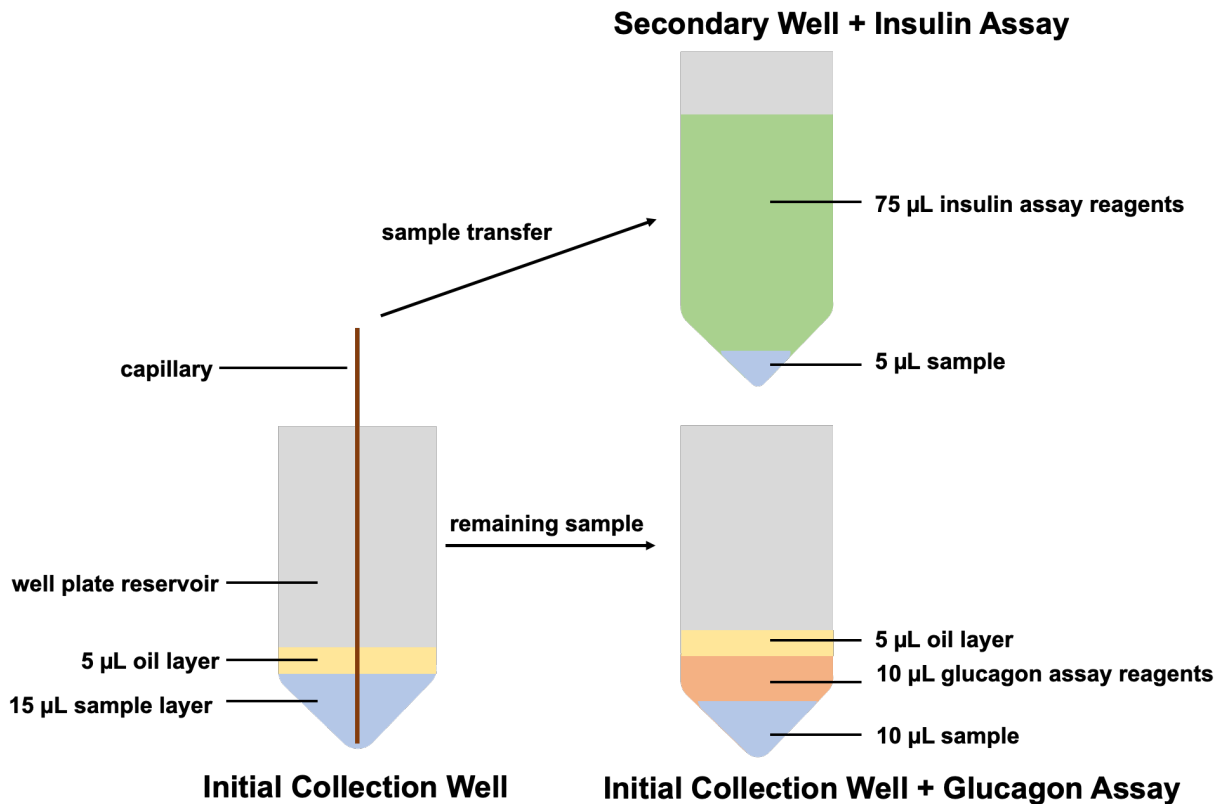


Figure 3-2. Diagram of capillary depositing sample into well with oil layer and the subsequent splitting of the sample.

Following the perfusion and sample collection from the device, the well plate contained 15 µL of sample and 5 µL of oil for every well used. This sample layer was subsequently split into two separate layers, for insulin and glucagon measurements using the FRET assays, as shown in **Figure 3-2**. Specifically, a 10 µL multi pipet transferred 5 µL of sample from the bottom of the initial collection wells (left, bottom) to a secondary well plate (top right) used for the insulin TR-FRET assay incubation. Following sample transfer to the new insulin well plates, insulin TR-FRET assay reagents were added, mixed well, and the resultant mixture was allowed to incubate in the dark for 12 hours. Similarly, glucagon assay reagents were added to the remaining 10 µL sample

and 5 μL oil left in the initial collection well plate (bottom right) and allowed to sit in the dark for a 12-hour incubation period.

Islets were removed from the device and lysed to measure the total glucagon content.⁶⁸ All islets were removed from the device by aspiration and placed into a 200 μL tube. The islets were then lysed following previously described methods.⁶⁸ The lysate was diluted 10:1 and 20:1 and pipetted into a 96 well plate in triplicate to measure total glucagon and insulin content.⁷⁵

TR-FRET Measurements for Glucagon and Insulin

The high range insulin assay was prepared to manufacturer specifications and the protocol for diluting stock reagents was followed.⁷⁵ In short, each plate had three replicates of 150, 60, 24, 9.6, 3.85, 1.54, 0.61 and 0 ng mL^{-1} standard insulin solutions made in BSS. Premixed reagents from the TR-FRET insulin assay kit (75 μL) were pipetted into each well using a 200 μL multichannel pipet. 5 μL of the 15 μL fraction were transferred to a secondary well for insulin measurement, the remaining 10 μL in the initial collection well was assayed for glucagon measurement (Figure 3-1). Plates were then sealed with a film and incubated in the dark for 12-14 hours. Following incubation, the plate was read using previously described methods. In short, TR-FRET measurement of the plate was performed to yield a ratio value. The FRET ratios presented are the average integrated emission at 665 nm to that at 620 nm multiplied by 10,000. For background correction, the average FRET ratio for the 0 ng mL^{-1} solution was subtracted from the average ratios for the standard solutions. Insulin calibration plots were generated by plotting the average FRET ratio for triplicate measurements of each standard insulin solution versus insulin concentration. The glucagon assay was prepared to manufacturer specifications. Well plates were read using previously described methods.⁷⁵ Each plate had three replicates of the standard glucagon solutions.

To test the dynamic response for the glucagon and insulin TR-FRET assays, the two flow reservoirs were filled with 5 mL of 3 mM glucose in BSS and either insulin or glucagon. Reservoir 1 had 1200 pg mL^{-1} and reservoir 2 had 9.6 ng mL^{-1} insulin. For 70 min, the flow was alternated between the two at 5 $\mu\text{L min}^{-1}$, 0-15 min glucagon with BSS was at 100% flow rate, 15-33 min insulin flow rate was at 100%, 33-51 glucagon flow rate was 100% and from 51-69 min the flow rate was 100% insulin. Based on the volumes of the channels of the device and of the outlet tubing, the time required for the analyte to travel from the mixing cross to the well was ~ 6 min. This time

was subtracted on the perfusion delivery profile and on all subsequent glucose islet perfusion traces.

Data Analysis

To quantify insulin and glucagon in each collected fraction, calibration curves were used to convert FRET ratios to concentration values. The cell lysate dilution in range of the calibration curve was used to quantify the total insulin or glucagon content. Plots showing secretion rate as a function of time are displayed as a percent of total, amount in fraction divided by the amount in lysate plus the sum of all fractions collected. The 15 min wash step when islets were added to the device is not accounted for in the percent calculation. The number of islets used in each experiment are in the text or caption of figure. Islets were counted and not converted to islet equivalent values.

Results

Introduction of a Light Mineral Oil to Prevent Evaporation

Sample evaporation throughout an experiment can lead to inaccurate result. For this study, fractions were collected over 80-90 minutes. However, a 15 μL sample will experience significant evaporation over this period, which can lead to increased concentration of hormone in measurements and therefore lower accuracy. Therefore, a thin layer of oil was used as an immiscible non-aqueous layer to prevent evaporation of a solution.

To ensure an oil layer would not interfere with the TR-FRET experiments, three replicates of the glucagon assay with and without an oil layer were incubated for 12 hours. The ratio of the two FRET signals (from control and oil-layer tests) was plotted for each concentration of the standard solution of glucagon (**Figure 3-3**). The average ratio of signals ($\text{FRET signal}_{\text{control}} / \text{FRET signal}_{\text{oil layer}}$) was 1.01 ± 0.05 for all data points (three replicates), showing no difference in the data across all concentrations. These results confirm that the addition of the oil layer in the well plate during fraction collection of the perfusate did not affect the peptides or the assay reagent. From this point, all glucagon data shown (e.g., calibrations and islet traces) were measured with 5 μL of light mineral oil atop the sample and reagents. The insulin well plates were not tested with oil because the sample used for the insulin assay was pipetted out of the original well plate (which had an oil layer) and added to a separate well plate, where it was then mixed with insulin assay reagents. Conversely, the glucagon assay reagents are added directly to the remaining sample

(which is still in contact with oil), which is why oil experiments were conducted with the glucagon assay. However, the insulin assay reagents were never exposed to the oil layer (Figure 3-1), and therefore oil layer tests were not performed for the insulin assay.

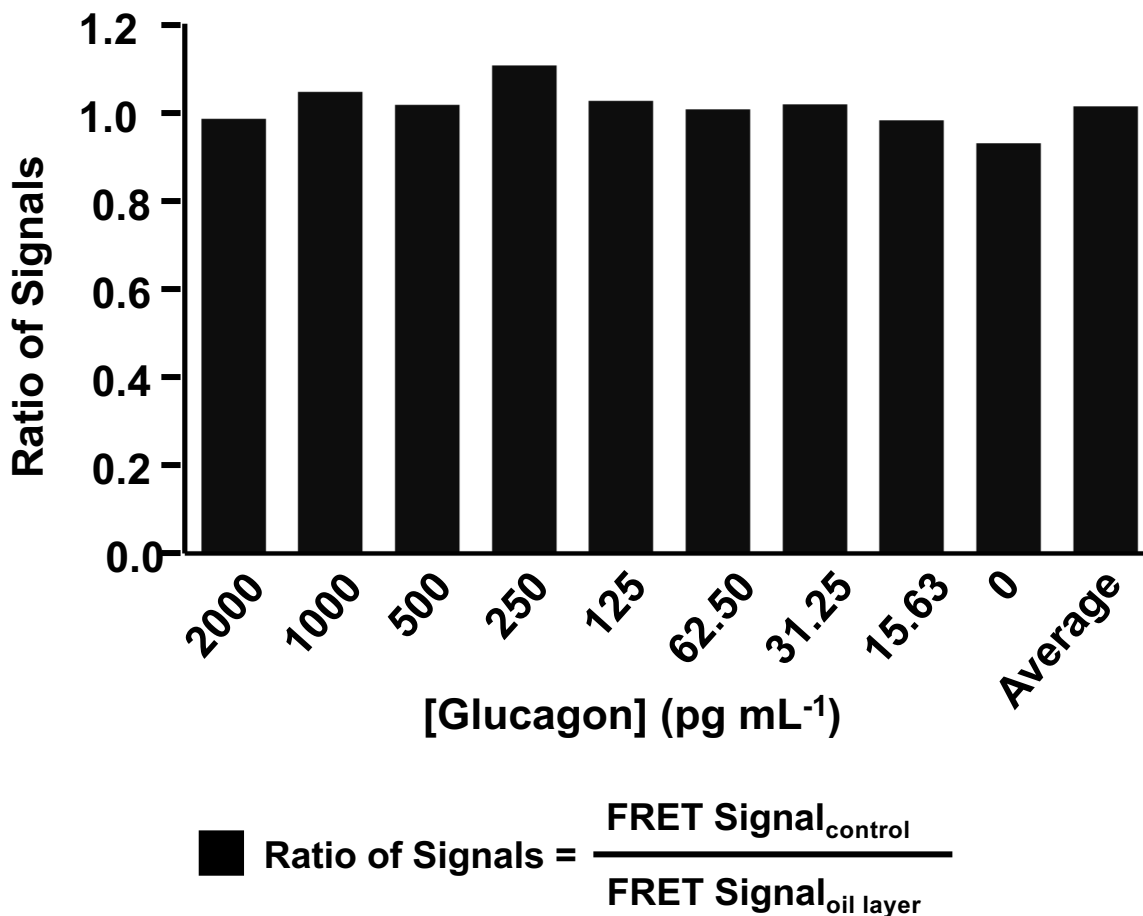


Figure 3-3. Comparison of assay signal of glucagon calibration incubated with layer of light mineral oil. Each assay was repeated in triplicate and both were incubated with a PCR cover on the same low volume well plate. After 12 hour incubation the TR-FRET value were measured and reported as a ratio for each concentration.

TR-FRET Calibration for Insulin and Glucagon

Calibration tests were performed for insulin and glucagon and their resultant traces are plotted in **Figure 3-4**. High range insulin assay calibration (left) had a range of 0.61 to 150 ng mL⁻¹ giving an LOD of 0.30 ng mL⁻¹. Glucagon TR-FRET assay (right) had a range from 15.6 pg mL⁻¹ to 2000 pg mL⁻¹ giving an LOD of 5 pg mL⁻¹. The relative standard deviation of the points ranged from 3.3 to 13.7% and 1.0 to 13.6% for insulin and glucagon, respectively. The concentrations of

these standard solutions determine the dynamic range the assays can be used for accurate quantification of these hormones using the assay. Estimated concentrations of glucagon and insulin secreted from batches of ~30 islets fall within these concentration ranges; thus, these assays were deemed suitable for accurate TR-FRET determination of insulin and glucagon secreted from human islets for the following experiments.

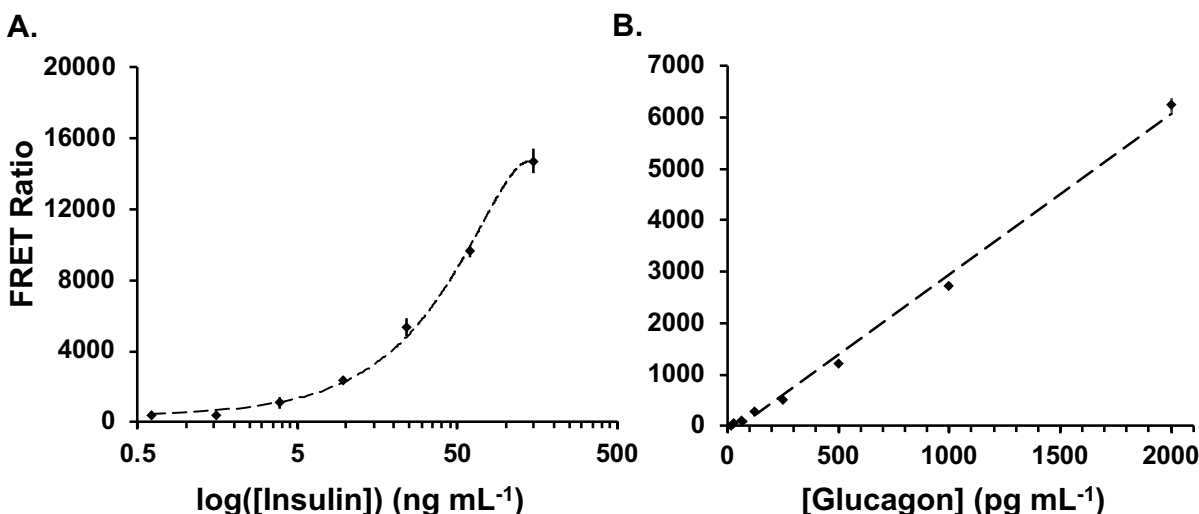


Figure 3-4. Insulin and glucagon TR-FRET assay calibrations. **(A.)** A representative of the insulin TR-FRET calibration is shown and **(B.)** a representative TR-FRET calibration of glucagon is shown. The points in both are an average of three replicates and the error bars are ± 1 SD.

The dynamic response of the device was determined through an experiment involving perfusion step changes of insulin and glucagon through the device. As shown in **Figure 3-5**, glucagon (white) was perfused for 18 minutes followed by an 18-minute perfusion of insulin (grey) and then repeated. Fractions were collected every three minutes and insulin and glucagon concentrations were measured using the TR-FRET assays; their concentrations are plotted in blue (glucagon) and red (insulin). As expected, when glucagon perfusion was 100%, detected glucagon (blue) was high (between ~78-95% of total expected response). However, for the second period of glucagon perfusion, the measured glucagon concentration was (only up to ~70%). The insulin quantification with the assay was better, because during periods of high insulin (grey), the measured insulin was above 80% during both pulses. It is important to note that a period of equilibration is required, so the concentrations of the earliest-collected fractions following a switch between insulin and glucagon (or vice versa) are generally lower than the final fractions collected during that period. Additionally, the insulin concentrations are very low during periods of 100%

glucagon perfusion; similarly, glucagon concentrations are also low during periods of 100% insulin perfusion. These results suggest that the assays are capable of detecting high versus low concentrations of insulin and glucagon.

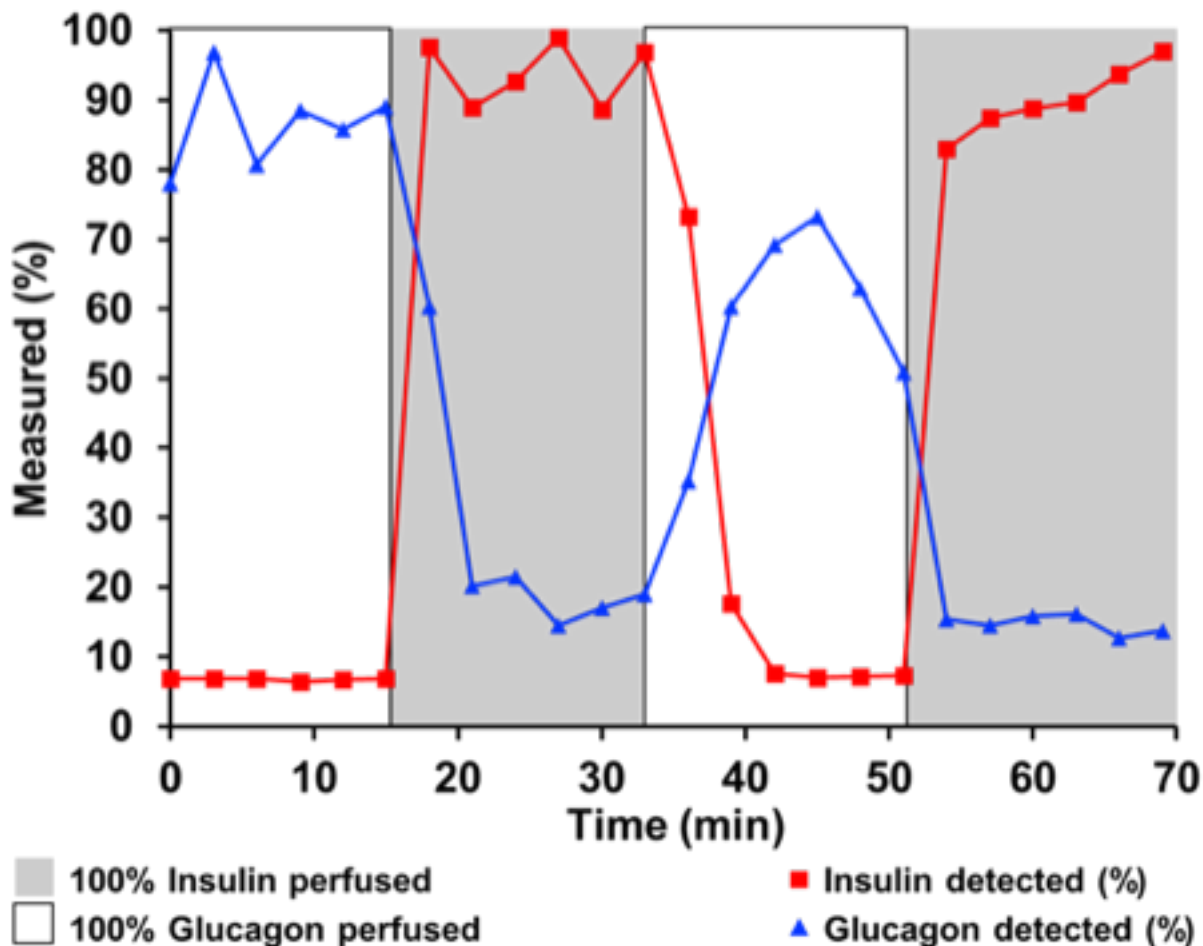


Figure 3-5. Flow dynamics. Dual perfusion system where blue indicates the level of glucagon and red the level of insulin being flowed into device by pressure system. White section is 100% glucagon and 0% insulin, grey is 100% insulin and 0% glucagon.

Following system performance tests, secretion from human pancreatic islets tested following perfusion of glucose. To perform the experiments, islets were initially placed in the microfluidic device, allowed to adhere for 10 min, and perfused with 5.6 mM glucose in BSS. After this period of basal release (9 min), the glucose level was increased to 16.7 mM (for 30 min), decreased to 5.6 mM (for 15 min), increased again to 16.7 mM (for 15 min), and finally decreased to 5.6 mM (for 15 min). Fractions were subjected to insulin and glucagon measurements using the FRET assays, and their resultant concentrations as a function of time are displayed in **Figure 3-6** for two sets of islets. As expected, when glucose concentrations increase (grey), insulin increased

and glucagon release decreased. Conversely, upon a decrease in glucose concentrations (white), glucagon concentrations increased whereas insulin concentrations decreased. Qualitatively, islets used in the experiments exhibited one of two patterns of release: either they showed a sustained level of release (Figure 3-6A), or a burst of glucagon secretion followed by a decline in the rate of release (Figure 3-6B), during the entire stimulation. These same two behaviors were observed for glucagon in Chapter 2. Due to the high variability in islet composition, secretion amounts were normalized to the total glucagon and insulin content in the islet population as described in the Materials and methods in Chapter 2. The glucose time curve was also adjusted by 3.0 min to account for the volume of the device and tubing.

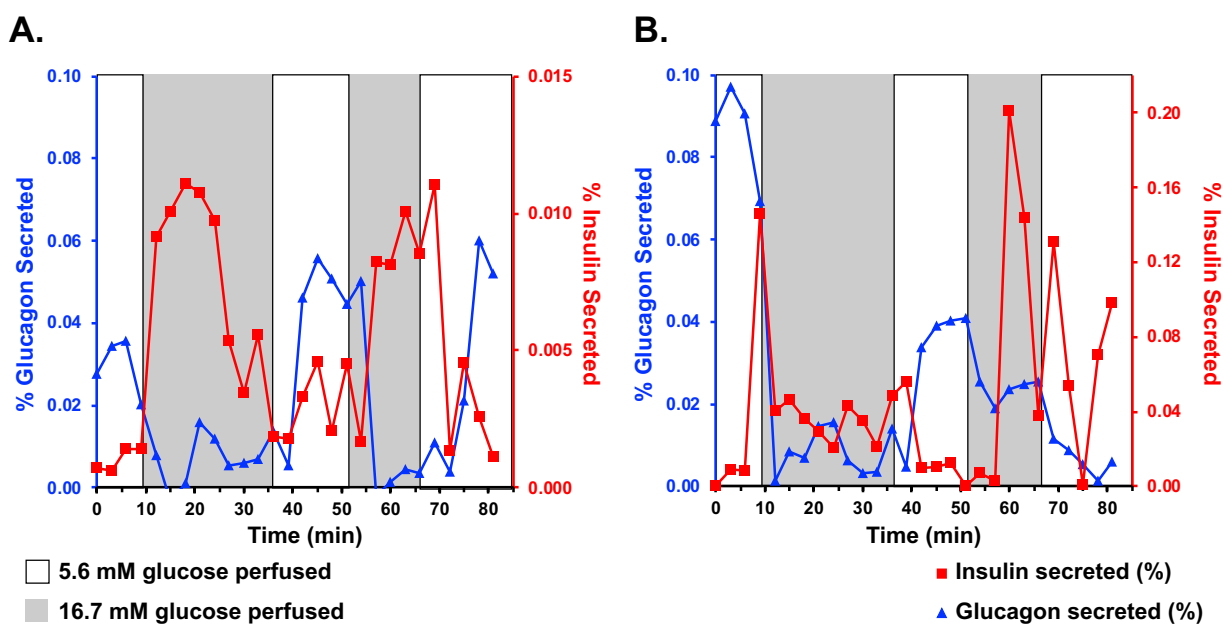


Figure 3-6. Human islet traces with dual peptide detection. Two traces are shown from a batch of human islets, while detecting both insulin and glucagon. The y-axis is the percent released of each, the total secreted measured and the total remaining in the islets after contributing to the percent value. The white section of the trace has a glucose value of 5.6 mM and the grey section has a glucose value of 16.7 mM. 30 islets were used for both traces shown.

The inverse relationship of insulin and glucagon is observed in both trace 1 and trace 2. Their out-of-phase behavior is observed during periods with high glucose concentrations in trace 2 (right, from 10 min to 40 min); insulin and glucagon concentrations (red and blue) oscillate out of phase throughout this time. The ability for this system to provide time-resolved measurements over short time periods (3 minutes) allows us to illustrate the behavior of these peptides. Furthermore, this sheds light upon the relationship between the two hormones. Interestingly, this

out-of-phase sinusoidal behavior is not observed for trace 1. Instead, trace 1 exhibits the “sustained release” behavior, along with changes in secretion rates when glucose levels are changed from high to low and from low to high.

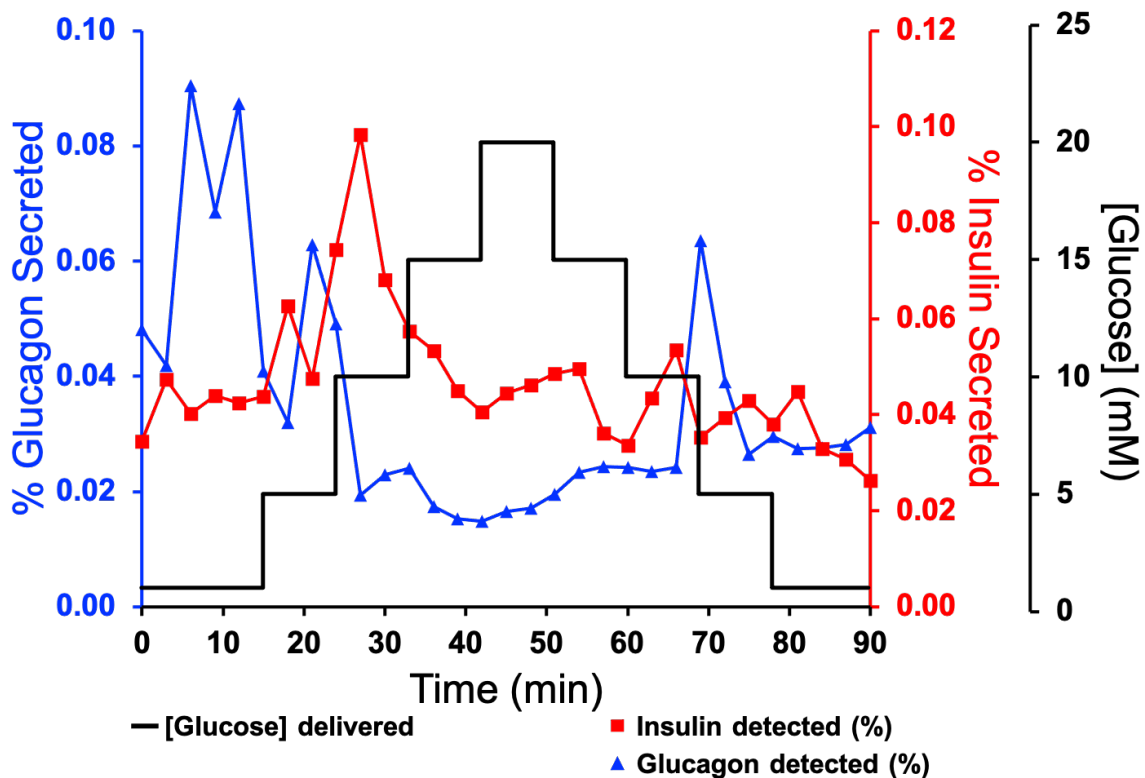


Figure 3-7. Human islet traces with dual peptide detection and dynamic glucose perfusion. The trace shown is from batch human islets (30 islets) in a microfluidic device. The y-axis is the percent released of each, the total secreted measured and the total remaining in the islets after contributing to the percent value. Glucose was delivered in a staircase fashion at 1, 5, 10, 15 mM and ending at 20 mM before returning down to 1 mM. Each concentration was held for 9 minutes so that three fractions could be collected during all intervals.

To probe the relationship between insulin and glucagon and to better understand their release behavior at different glucose concentrations, a study using a “staircase” of glucose (at different concentrations) was delivered to the microfluidic device containing human islets and the amount of hormone released was quantified with the FRET assays. The glucose staircase is shown in **Figure 3-7** (black) along with the insulin (red) and glucagon (blue) concentrations at each 3-minute time point. Glucose concentrations started low (1 mM) for 15 minutes and then increased every 9 minutes (to 5, 10, 15 mM glucose). Then glucose was lowered step-wise in a similar fashion every 9 minutes before returning to a low glucose concentration (1 mM). Insulin (red) spiked after the first increase in glucose (15-24 minutes) and again for the second increase (24-33

minutes). However, insulin secretion then slowly decreased until the glucose concentration returned to 10 mM, when it exhibited a small spike again. Small oscillations in insulin concentrations were then observed for the rest of the experiment. Glucagon concentrations were high during the 1 mM glucose period and then was briefly muted upon the first increase in glucose (to 5 mM), followed by a small spike in glucagon until the next increase in glucose (to 10 mM), when it dropped again. Glucagon concentrations then remained low until it spiked at the 70 mi fraction, when glucose was decreased to 10 mM; glucagon concentrations then decreased again for the remainder of the experiment. For both insulin and glucagon, the 10 mM glucose stimulated spikes/drops in release.

As previously mentioned, insulin and glucagon have opposite roles in that they decrease and increase blood sugar in response to glucose concentration changes. This experiment illustrates the poorly-understood sinusoidal release patterns for insulin and glucagon. This is specifically observed from 15-35 minutes, where a spike in one hormone concentration is accompanied by a drop for the other. For periods of high glucose, the sinusoidal behavior is not observed, however it is again observed from 60-90 minutes, with lower amplitude of oscillations.

The percent of glucagon and insulin secreted during the glucose dose staircase was quantified and normalized to the stimulation period (9 minutes) to yield average secretion rates for each glucose dose. The average secretion rates for the high and low glucose study (Figure 3-5) and staircase dose study (Figure 3-6) are shown in the plot in **Figure 3-8**, with the average shown as a shape (square or triangle) and the error bars corresponding to ± 1 SD. For the high and low glucose study (Figure 3-7, left), the average insulin release during 16.7 mM perfusion was ~ 3 times higher at $0.036 \pm 0.025\% \text{ min}^{-1}$ than the measured release during 5.6 mM glucose, $0.013 \pm 0.009\% \text{ min}^{-1}$. The average glucagon release during the 5.6 mM glucose was ~ 3.5 times higher at $0.035 \pm 0.027\% \text{ min}^{-1}$ than the measured release during 16.7 mM glucose perfusion, $0.011 \pm 0.013\% \text{ min}^{-1}$.

For the dose staircase (data shown in Figure 3-7), the averages for repeated doses (on the way “up” and “down”) were calculated by combining all the data points from the same glucose concentration (on either side of the glucose staircase). Overall, the glucagon release in the dose staircase experiment (Figure 3-8, middle) exhibits linear behavior and decreases with increasing glucose concentration. Additionally, the 10 mM glucose is an inflection point due to the high standard deviation. Conversely to glucagon release, the insulin plot (Figure 3-8, right) shows a

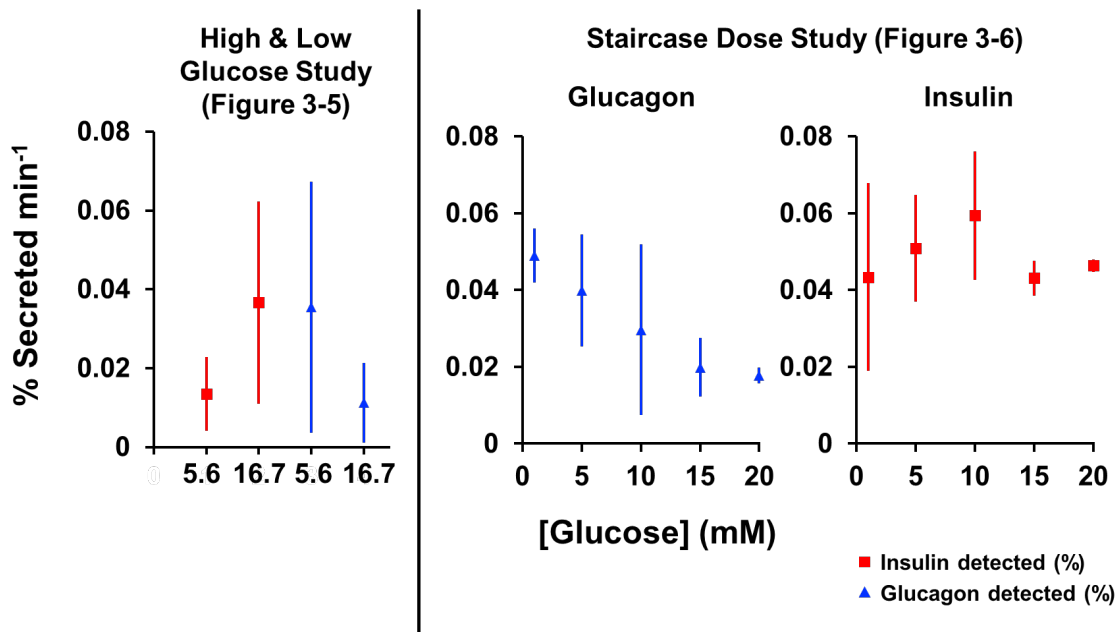


Figure 3-8. The total glucagon (blue) and insulin (red) secretion levels normalized over the collection time (total glucagon or insulin min⁻¹) for both traces shown in Figure 3-6 (left). Average secretion levels normalized over collection time for glucagon and insulin are shown (middle and right) over a glucose staircase dose delivery from Figure 3-7.

steady increase with increasing glucose from 1 mM to 10 mM and a steady response from 15 mM and 20 mM glucose. An obvious inflection point is not observed for insulin.

Conclusion

The ability to measure trace amounts of insulin and glucagon released from human pancreatic cells is demonstrated using microfluidic device and a novel TR-FRET immunoassay. Similarly to what was observed for glucagon in Chapter 2, there are two behavior profiles observed for glucagon released from human islets when blood glucose drops: a burst or a sustained release of glucagon. Furthermore, this study demonstrates a similar behavior for insulin; when glucagon follows the “burst” profile, insulin does as well (when blood glucose increases). However, if glucagon follows the sustained-release profile during periods of low glucose, insulin also will behave with the sustained-release pattern. Additionally, this study illustrates the out-of-phase sinusoidal behavior for insulin and glucagon; the release of these hormones from pancreatic human cells over short time periods has not been extensively studied; information regarding their relationship can improve understanding of diabetes. The oscillatory out-of-phase relationship for

insulin and glucagon is not observed at high concentrations of glucose, and is most obvious for concentrations from 1-10 mM.

Automated fraction collection system with the ability to collect low volume samples over long periods of time has proven useful and effective for small cell sample analysis. The TR-FRET assay can be performed without washing steps, it makes a strong candidate to be implemented for online detection of insulin and glucagon. The improvements in the system described here will be of interest to other field and applicable to similar fraction collection-based systems.

CHAPTER 4

SUMMARY AND FUTURE DIRECTIONS

Summary

A microfluidic system has been developed and characterized for quantitative glucagon secretion measurements from a batch of human pancreatic islets. Modeled experimental conditions ensured an experimental environment that would not be damaging to the islets in the device, focusing on the shear stress experienced by the islets. To demonstrate the utility of the system batches of human islets were loaded in the device and perfused with variable glucose concentrations to stimulate islet peptide secretion. Islets from 5 different cadaveric donors were tested using this system. Two different patterns were distinguished from the secretion profiles, “burst” and “sustained” release of glucagon. Further investigating of this pattern and improvement of analytical methods to reduce the number of islets in the device to preserve any secretion patterns that could be lost when looking at a group of islets.

Improvements in the system an improved perfusion microfluidic device, fluidic flow system, fraction collection system and implemented a second TR-FRET assay to measure insulin release from human islets as well as glucagon. The microfluidic device reduced the channel dimensions and added a second inlet for on chip mixing of two fluids. The fluid flow system was changed from a mechanically driven syringe pump to a pressurized fluid system with a feedback mechanism for consistent fluid flow rates. A CNC machine was programed to collect fraction in a low volume well plate, reducing the variability of manual fraction collection. Additionally adding a second TR-FRET assay specific for insulin will give twice the hormone release information that before. These improvements are laying the foundation to move this developed system towards a lab on a chip device that can encompass a dynamic perfusion system, islet chamber, total collection of secreted peptides from cells and online analysis.

Future Directions

It has been shown that the TR-FRET assay can be used to measure glucagon and insulin in a well plate. While this system can accommodate about 30 islets, which, is a much lower number than islets experiments commonly done in the field, the focus is towards single islets.

Single islet interrogation is able to capture the release dynamics of glucose regulating hormones, this has been shown for insulin where a group of islets will show a sustained increase in insulin released during a period of increased glucose, when there is only a single islets the insulin release dynamics are oscillatory. A single islet secretion measurement can only be made when two important goals are met, first the measurement must be sensitive enough to detect the low amount of the analyte of interest and second the measurement must have a time resolution fast enough to observe the dynamic changes in secretion rates over time.

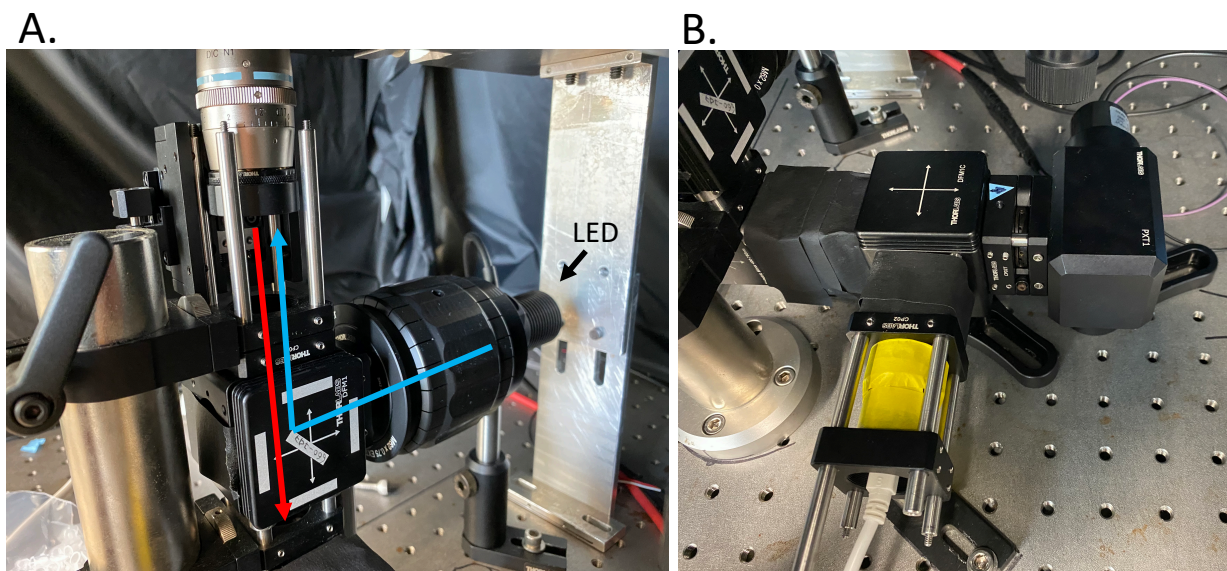


Figure 4-1. The custom optical system built to make FRET measurements. (A.) The LED and collimator obtained from Thorlabs was controlled by a time to live signal outputted from a DAQ card connected to LabView. The light is collimated and directed into a dichroic mirror and up through the back of the 40x Nikon objective. Fluorescence is then collected by epifluorescence and directed towards the photon measuring system (B.) The collected light is passed through an iris and emission filters before the photomultiplier tube.

The first goal of this is the measurement of low amounts of analyte. Using the TR-FRET assay the limits of detection are well within the range of insulin and glucagon that would be observed being released from an islet. That leaves the sensitivity of the measurement to be limited by the optical detection system. The complicated features of a FRET detection system include a powerful pulsed light source and two PMTs with a rapid response time to detect emission from the donor and acceptor fluorophore over the measurement window.

A custom PMT was wired and integrated into a Thorlabs cage optical system shown in **Figure 4-1.** The PMT has a response time of 2 ns which is more than fast enough for FRET

measurements. To properly measure FRET, two PMTs are needed, for preliminary testing of the system and assay, one PMT was used to monitor the acceptor emission at 665 nm. The acceptor emission intensity was directly proportional to the FRET ratio of the sample, but less quantitative. The current output from the PMT bulb was fed to a current to voltage converter, which acts to amplify and filter the signal prior to recording a value on the DAQ card. The DAQ card used has a maximum acquisition frequency of 250 kHz corresponding to one data point every four μs . This acquisition would be fast enough to develop a system to make TR-FRET measurements.

The other goal in making these measurements to make the measurements with a high time resolution so that any dynamic release of secreted peptides can be observed. Utilizing microfluidics can facilitate time resolved measurements. A common approach to prevent band broadening in microfluidics is to use droplets, this segments the fluid in an inadmissible oil phase. Oil droplets can then be supplemented with assay reagents, transferred to external tubing for assay incubation and directed towards a measurement system.

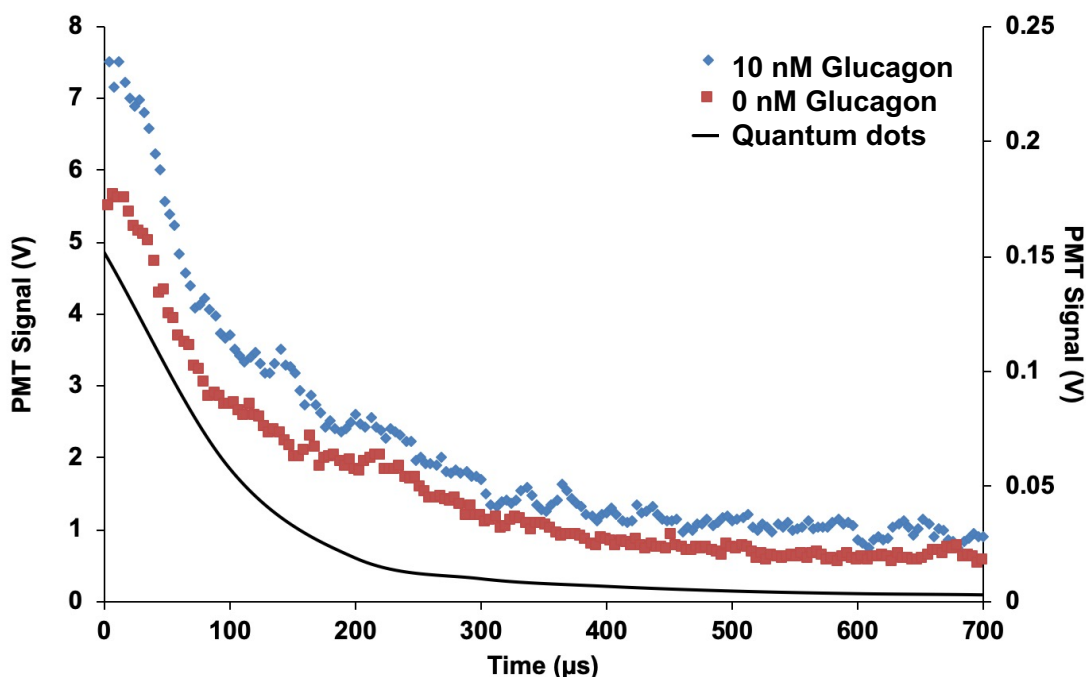


Figure 4-2. Glucagon positive control test. The right axis corresponds to the quantum dot signal during the off cycle of the LED. The left axis corresponds to the glucagon 0 nM and 10 nM standard solutions used to test the TR-FRET measurement of the system.

To test the LED excitation pulses and the photon detection system TR-FRET assay was loaded into a capillary and measured, shown **Figure 4-2**. The LED signal shown on the right axis

demonstrates a decay time that is 100s of μs long, and can be seen past 300 μs . Excitation light seen in the measurement window will hinder FRET measurements by increasing the background of the sample. A 10 nM and a 0 nM standard solution glucagon were mixed with TR-FRET assay reagents and loaded into a capillary to measure the FRET signal. Each data point represents 50 averaged runs for each concentration. Each run was recorded using the same LED power and PMT voltage. The solution with 10 nM glucagon exhibited a higher signal through measurement window.

The preliminary testing has proved promising that this TR-FRET assay can be detected in a much lower volume than in a well plate and record a difference in signal between 10 and 0 nM glucagon. With improved pulse excitation light by a motorized chopper or with a flash lamp and with a second PMT to monitor the donor wavelength, this system will be primed to make time resolved glucagon measurements from human islets of Langerhans online.

APPENDIX A

SIMULTANEOUS MEASUREMENTS OF REACTIVE OXYGEN SPECIES (ROS) WITH INSULIN SECRETION FROM ISLETS OF LANGERHANS

Summary

Reactive oxygen species (ROS) play a critical role in the function of pancreatic β -cells within islets of Langerhans. The production of these species has been linked to both cellular stress and regulation of insulin secretion. Therefore, it is crucial to delineate the acute temporal relationship between ROS generation and insulin release dynamics. In this study, a microfluidic system was used for simultaneous measurements of Grx1-roGFP2, a redox-sensitive biosensor, with insulin release patterns from single murine islets every 10 s. The biosensor was selectively expressed in β -cells and used with islets that were exposed to acute delivery of alloxan monohydrate, a toxic glucose analog that induces ROS generation, or step increases in glucose concentration. Delivery of these agents resulted in increased biosensor fluorescence, indicative of increased ROS levels. To measure redox dynamics and their association with insulin release patterns, single islets were exposed to an acute challenge with 11 mM glucose while the biosensor fluorescence was imaged simultaneously with insulin levels measured using a competitive immunoassay. The resulting secretory profile of insulin was biphasic, in which the first phase response was observed with a duration of 5-10 min, followed by second phase oscillations with periods of 3-5 min. The biosensor fluorescence exhibited similar dynamic profiles, with the fluorescence rapidly increasing during first phase insulin release and showing pulsatility that was highly synchronized with insulin oscillations during second phase release. These results point to a tightly coupled association of ROS and insulin release during acute glucose stimulations.

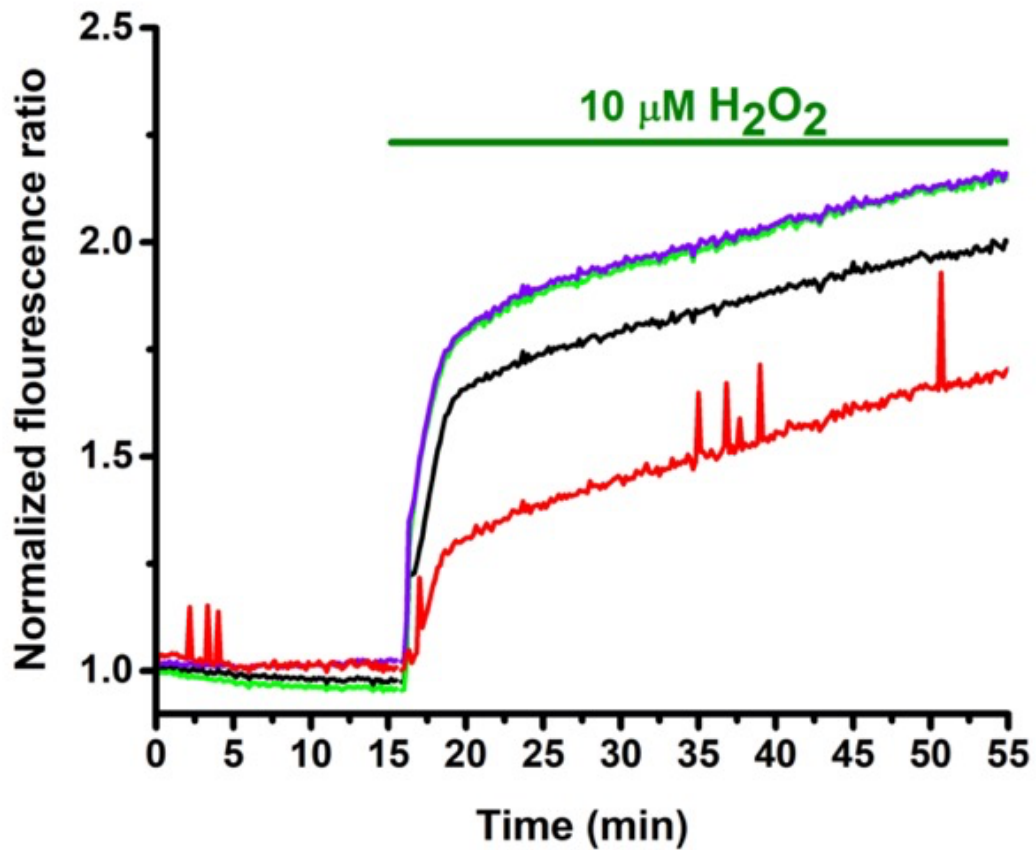


Figure A-1. H₂O₂-induced increases in Grx1-roGFP2 fluorescence. Five biosensor-expressing islets were held in a glass-bottomed dish containing BSS with 3 mM glucose. Fluorescence was measured from the biosensor every 10 s and is plotted on the left y-axis. H₂O₂ was spiked into the dish to a final concentration of 10 μM at the time indicated by the horizontal bar.

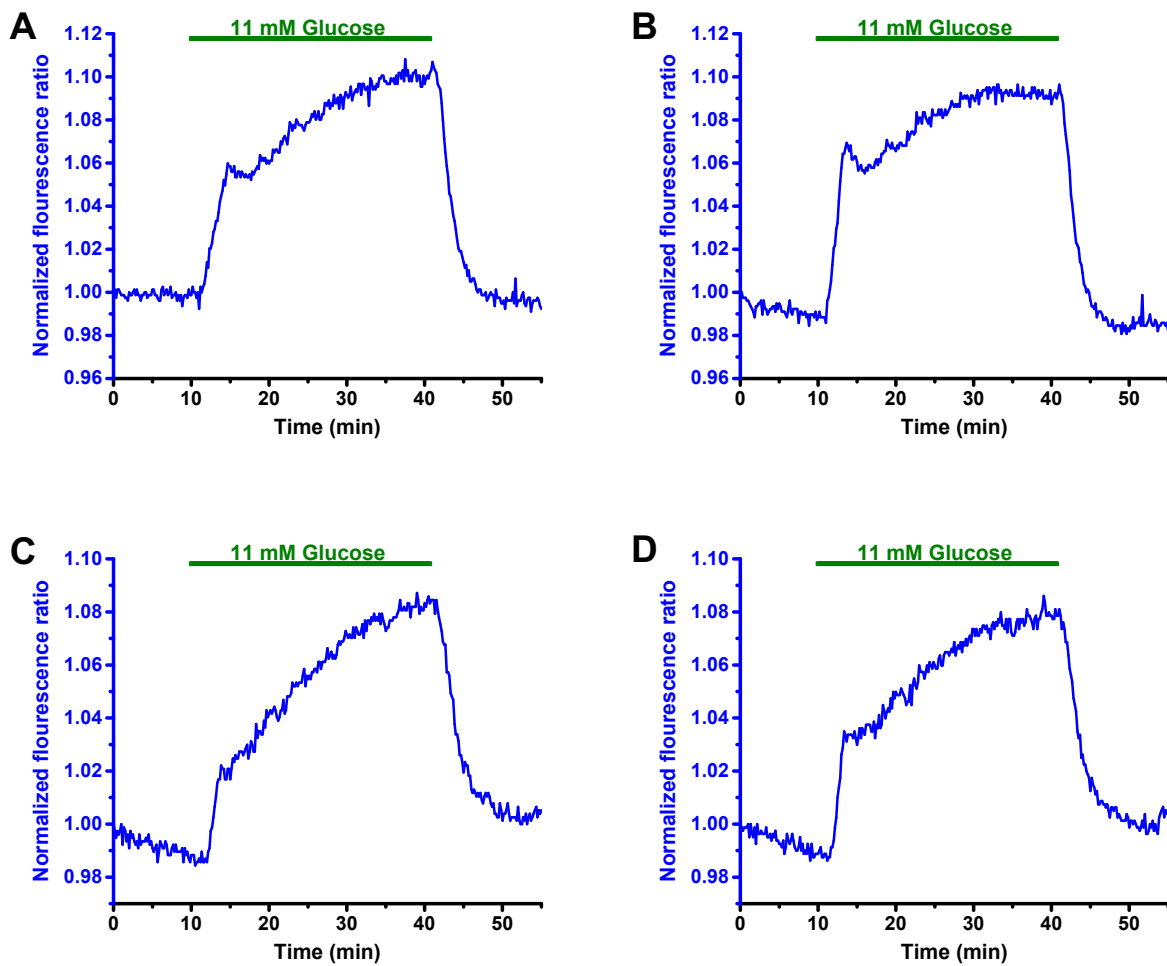


Figure A-2. Acute delivery of 11 mM glucose. Grx1-roGFP2-expressing islets were initially perfused with 3 mM. The glucose concentration was increased to 11 mM during the time shown by the horizontal bar on the tops of the figures. The glucose level was returned to 3 mM for the final 10 min of recording.

APPENDIX B

DEVELOPMENT OF A CUSTOM OPTICAL SYSTEM FOR INSULIN MEASUREMENT FROM A SINGLE ISLET OF LANGERHANS

The amount of insulin released from an islet depends on the volume of the microfluidic system used, but typical ranges are 10 to 300 nM. Detecting other glucose regulatory hormones is more problematic because the levels of glucagon, somatostatin, and ghrelin released from islets are 10-100 times less than the amount of insulin. The immunoassay used for insulin can measure in the low nanomolar range, but is not capable of the picomolar detection needed for these other analytes.

There are two types of immunoassays that are often used to target an analyte in a microfluidic system, a competitive immunoassay and a noncompetitive immunoassay. The competitive immunoassay has an affinity probe, usually an antibody (Ab), and a marked antigen (Ag*), usually fluorescently labeled. Ab and Ag* are mixed with the unlabeled antigen of interest (Ag). Both Ag* and Ag compete for binding sites on the Ab present in solution:

Competitive assays: $Ag^* + Ag + Ab \rightleftharpoons Ab-Ag^* + Ab-Ag + Ag^* + Ag$

The noncompetitive assay utilizes a labeled affinity probe (Ab*) in a high concentration to shift the equilibrium to the right, thus chelating all Ag to the Ab*:

Noncompetitive assays: $Ag + Ab^* \rightleftharpoons Ab^*-Ag + Ab^*$

When characterizing the products of these immunoassays, the Ab*-Ag or Ab-Ag* complex is referred to as “bound” (B) when compared to the uncomplexed species Ab* or Ag* which is referred to as “free” (F).

The competitive assay relies on a strong binding affinity between the Ab and the Ag. The limit of detection for a competitive assay is limited by the binding affinity, K_d . A typical K_d for an IgG monoclonal antibody ranges from low nM to high picomolar.⁸⁰ A noncompetitive assay is less

affected by the binding constant and is usually limited by how well the optical system can measure the Ab*-Ag complex.

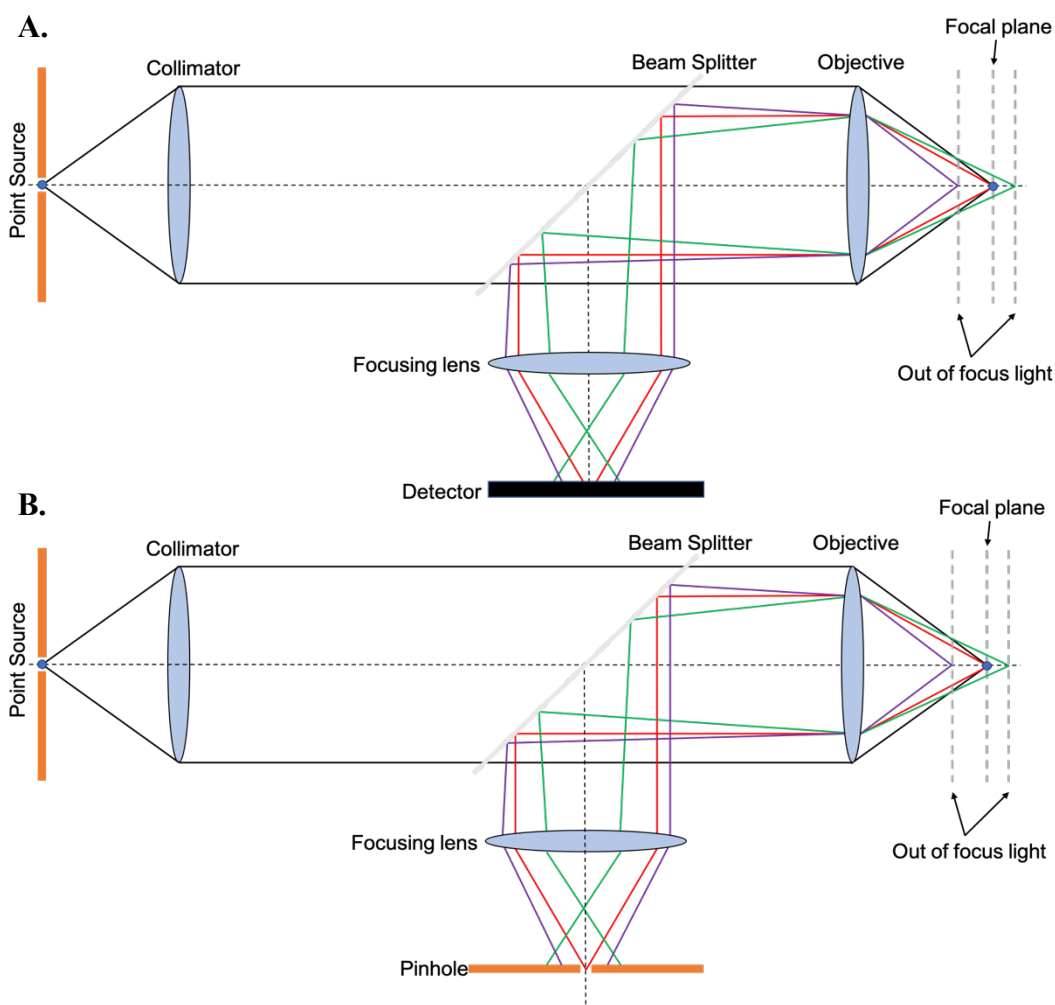


Figure B-1. (A) Schematic of a wide field epifluorescence microscope, where one microscope objective is used for sample illumination and detection. The purple and green light trace represent excitation light that is scattered back through the objective and read by the detector. (B) Schematic of a confocal microscope. The focusing lens completes the confocal geometry to selectively image a single point within a thick sample.

Measurements of a competitive immunoassay are done with a wide field epi-fluorescence, shown in **Figure B-1 (A)**. Both the excitation and detection are on the same side of the sample which allows for the use of a single microscope objective. With these systems, typical limits of detection (LOD) are $10^{-9} - 10^{-10}$ Molar. This will handicap a noncompetitive immunoassay targeting analytes below the LOD.

In contrast, confocal microscopy rejects out of focus light collected by the objective, as shown in **Figure B-1 (B)**.⁸¹ The confocal geometry reduces the amount of back scattered light through the objective.⁸² The out-of-focus light in green and purple is not collimated by the objective, resulting in either diverging or converging light when it reaches the focusing lens. Only collimated light that reaches the lens will be focused through the objective; all out-of-focus light will be focused before or after the pinhole.

This approach decreases the baseline and, as a result, decreases noise. There are three main types of electrical noise, white noise, flicker noise and shot noise. White noise and flicker noise create a relatively small noise signal when compared to shot noise. Shot noise is a fundamental noise that scales with the square root of signal intensity. Blocking the scattered excitation photons decreases the baseline number of photons that are read by the PMT, resulting in a baseline close to zero with significantly less shot noise. Low noise readings result in high signal to noise measurements which lead to low LODs. A confocal detection system has been used to obtain a 300 fM detection limit from electrophoretic separation of fluorescein on a microfluidic device.⁸¹

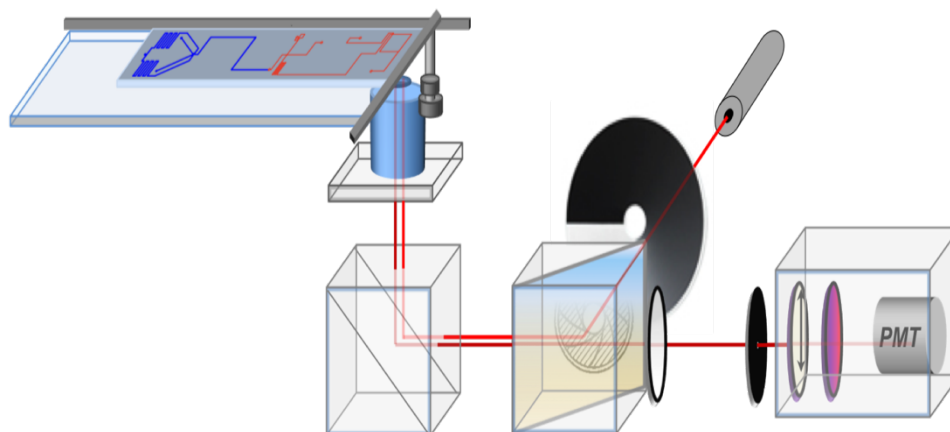


Figure B-2. Schematic of the detection system for laser induced fluorescence adapted. The red lines represent the path the laser light takes to the microfluidic device and the fluorescence path from the separation channel to the photomultiplier tube.

This system, shown in **Figure B-2**, was built and utilized a 633 nm diode laser that passed through a gradient neutral density filter to adjust the laser power. The beam size is controlled by an iris placed before the dichroic mirror. A steering mirror was used to direct the light to a 40X 0.6 NA extra-long working distance objective. The 633 nm laser light was made incident on the

microfluidic channel at the detection point. Fluorescence was then collected by the same objective and collimated. The light passed through the dichroic mirror toward a focusing lens. The lens focused the light through a 1000 μm pinhole mounted on a XY positioner. Only the light from the focal plane was focused onto the pinhole; all other scattered light collected by the objective was rejected by the pinhole. The light passed through the pinhole and an emission filter before reaching the photomultiplier tube (PMT). The current output from the PMT is converted to a voltage by an operational amplifier. The resulting voltage is read by a data acquisition card and recorded by a LabVIEW program written in-house.

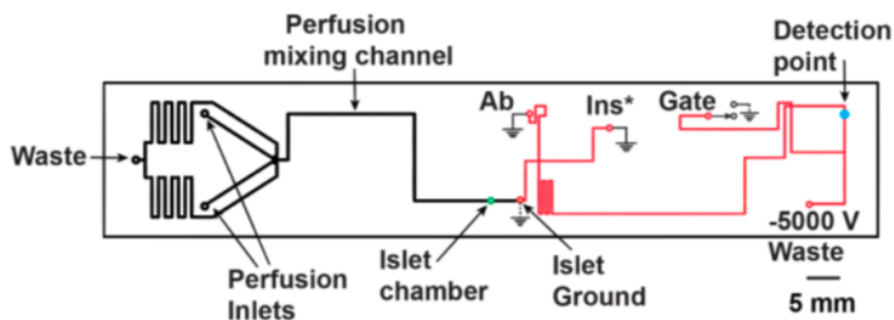


Figure B-3. Microfluidic device design incorporates two different flow components. The black line represent channel where gravity driven flow occurs. The red line shows where electroosmotic flow drives the liquid from the grounded inlets to the -5000 V waste outlet.

The microfluidic device schematic is shown in **Figure B-3**. The design allows for the entire experiment to be carried out inside the fluid channels of the device. Two inlets for the perfusion part of the device allows for varying concentrations of stimulant to mix and be delivered to the sample, in this case an islet. The perfusion channels are etched 30 μm deep. Hydrostatic pressure is achieved by elevating the syringes above the microscope stage on a stepper motor-controlled pulley system. In response to the delivered stimulus, the secretions are captured and mixed online with immunoassay reagents by electroosmotic flow (EOF). The insulin immunoassay is selective to insulin, so there is no cross reaction with other hormones released. The immunoassay reagents are mixed and incubated online at 37° C before an injection every 10 seconds into the separation channel. The separation channel is 10 cm long and takes about 6 seconds to separate the bound $\text{Ag}^*\text{-Ab}$ from the free Ag^* . The constant flow conditions allow for continuous monitoring of biological samples over time.

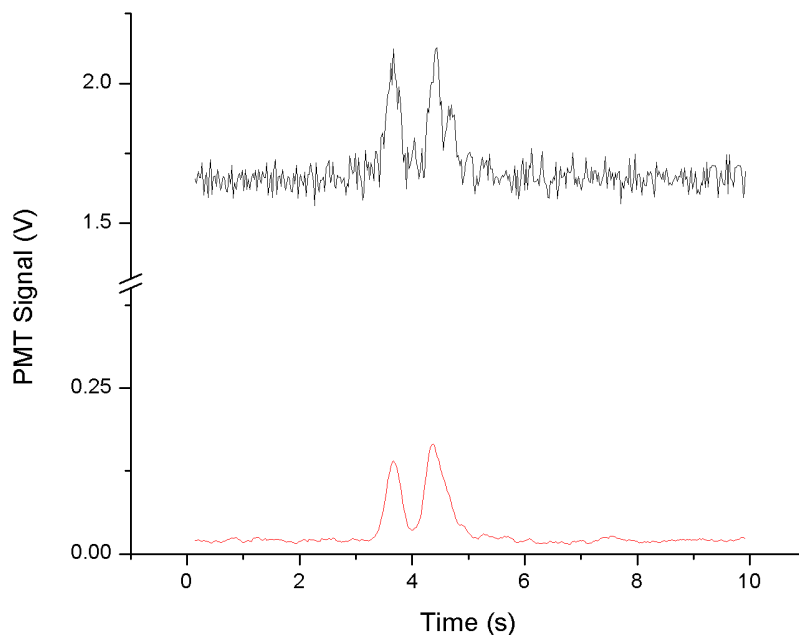


Figure B-4. A electropherogram comparison between a wide field (black) measurement and a confocal measurement (red).

In order to ensure the confocal system was rejecting the out-of-focus light, the optical system was tested using a competitive assay. The electropherograms of the insulin immunoassay separation on the microfluidic chip are shown in **Figure B-4**. To compare the confocal system to a conventional wide field system, the separation was done with and without the pinhole to demonstrate an improvement in the signal-to-noise ratio. The pinhole successfully rejects the scattered laser light from reaching the PMT as seen by the baseline drop from over 1.6 V to about 0.02 V. The RMS drops from 0.033 V to 0.0023 V. The PMT voltage was held constant at -800 V with the same laser power for each run. A baseline close to zero allows signal amplification without greatly changing the baseline. This approach increased the signal-to-noise readings by over 6 times the original.

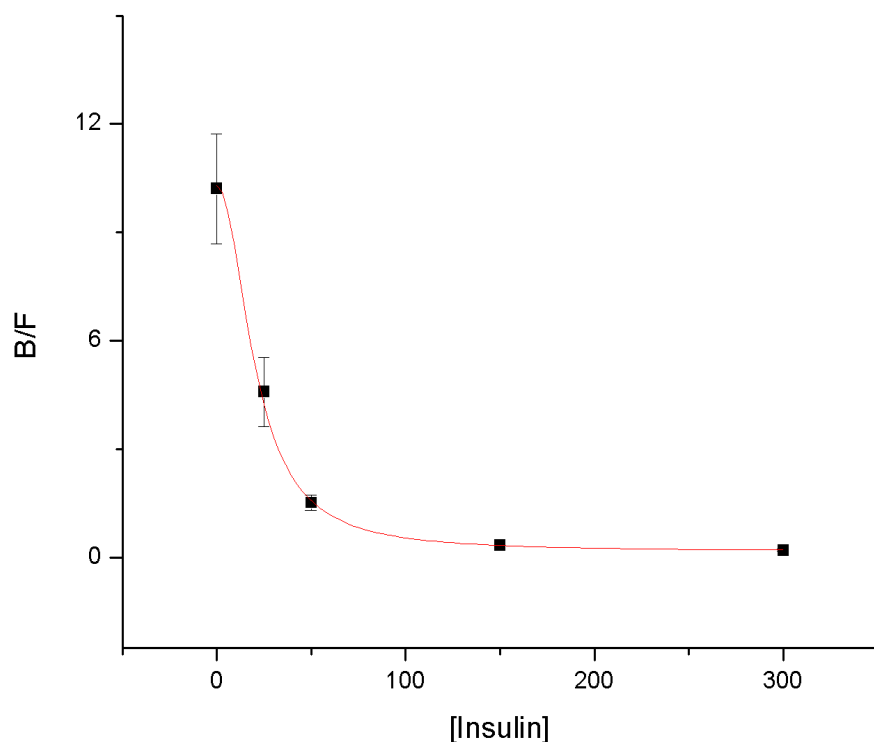


Figure B-5. An insulin competitive immunoassay calibration curve, increasing the amount of insulin consequently decreases the amount of insulin-cy5 that is bound to the antibody. There is an inverse relationship between the B/F ratio and insulin concentration (nM).

The goal of the confocal system was to be able to measure insulin by way of a competitive immunoassay. It was paramount to make reproducible insulin measurements. To ensure the system could accurately quantify insulin concentration in solution, an online calibration was performed. The reagents were mixed online and incubated in the mixing channels before detection. The two reagents with a fixed concentration were the insulin monoclonal antibody and the fluorescently labeled insulin-cy5. Both were prepared to have a concentration of 150 nM. Because there are three channels that combine into the mixing channel, the effective concentration is a third of the prepared solution. This gave a concentration of 50 nM for the known reagent and one-third dilution of any biological sample captured by the EOF channel. As described previously, the only components of a competitive immunoassay that are detectable via LIF are the antibody and labeled antigen complex and the free antigen, which in this case would be the Ab-Ins* and Ins*. The calibration shown in **Figure B-5** is a result of 15 electropherograms for each data point, the average

B/F and standard deviation is taken from the set. This assay routinely gave a limit of detection for insulin below 10 nM, more than what is needed when interrogating single islets on this platform.

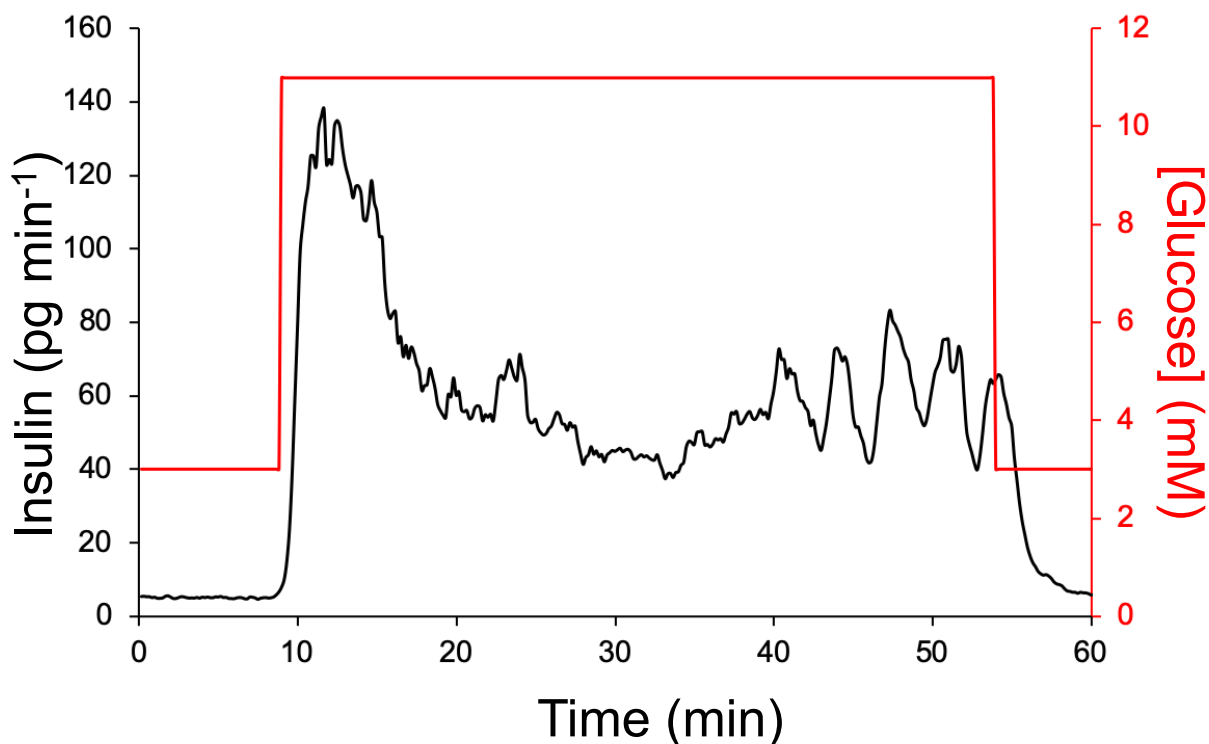


Figure B-6. Single islet insulin detection using confocal system. The separation immunoassay was used in a competitive format. Glucose stimulation was from 3 mM to 11 mM for 45 min and back down to 3 mM.

The optical system and microfluidic device were used to monitor insulin released from an islet during a glucose stimulation shown in **Figure B-6**. The initial first phase is observed when glucose is increased. The first phase of insulin release is documented in the literature when glucose levels increase. The islet then is observed to have release insulin for the next 25 min with no oscillatory pattern. At the 40 min mark the islet start to release insulin in an oscillatory fashion, demonstrating that this system can sensitively measure insulin released from single islets while maintaining the release pattern from the cells.

APPENDIX C

ABBREVIATIONS

Förster-resonance energy transfer (FRET)

Weight percentage (wt%)

Glucose-stimulated insulin release (GSIS)

Body mass index (BMI)

Enzyme linked immunosorbent assay (ELISA)

Radioimmunoassay (RIA)

Probe (P)

Probe target (T)

Capillary electrophoresis (CE)

Limit of detection (LOD)

Balanced salt solution (BSS)

Dissociation constant (k_d)

Temperature (T)

Viscosity (η)

Density (ρ)

Volumetric Flow Rate (V)

Standard deviation (SD)

Computer numerical control (CNC)

Reactive oxygen species (ROS)

Photomultiplier tube (PMT)

Electroosmotic flow (EOF)

Antibody (Ab)

Marked antigen (Ag*)

Unlabeled antigen (Ag)

affinity probe (Ab*)

Bound (B)

Free (F)

APPENDIX D

ANIMAL CARE AND USE COMMITTEE ASSURANCE LETTER



FLORIDA STATE
UNIVERSITY

ANIMAL CARE AND USE COMMITTEE [ACUC]
101 BIOMEDICAL RESEARCH FACILITY
TALLAHASSEE, FL 32306-4341
TELEPHONE: 644-4262 FAX: 644-5570
MAIL CODE: 4341

November 17, 2021

The Graduate School
Florida State University

To Whom It May Concern:

Concerning the thesis/dissertation submitted to the Graduate School by:

Graduate Student: Wesley Eaton
Thesis/Dissertation Title: Monitoring Peptide Secretion Dynamics from Human Pancreatic Cells Using a Sandwich Assay and Microfluidics
Department: Chemistry and Biochemistry
Major Professor: Dr. Michael Roper

The graduate student named above has provided assurance to the FSU Animal Care and Use Committee that all animal procedures utilized in work resulting in this thesis/dissertation are described in FSU ACUC Protocol(s):

Protocol Number	Title	Date ACUC Approval
1813	Procurement of islets of Langerhans	04/25/2018
202000078	Procurement of islets of Langerhans	12/10/2020

The Animal Care and Use Committee has confirmed that this student was included as a project member during the period covering their thesis/dissertation work. This institution has an Animal Welfare Assurance on file with the Office for Laboratory Animal Welfare. The Assurance Number is D16-00491 (A3854-01).

Sincerely,

ACUC Veterinarian
FSU Animal Care and Use Committee

KMH/kjj

cc: Wesley Eaton
Dr. Michael Roper

REFERENCES

- (1) Gaisano, H. Y.; MacDonald, P. E.; Vranic, M. Glucagon Secretion and Signaling in the Development of Diabetes. *Front. Physiol.* **2012**, *3 SEP* (September), 1–12. <https://doi.org/10.3389/fphys.2012.00349>.
- (2) Skjaervold, N. K.; Knai, K.; Elvemo, N. Some Oscillatory Phenomena of Blood Glucose Regulation: An Exploratory Pilot Study in Pigs. *PLoS One* **2018**, *13* (4), 1–13. <https://doi.org/10.1371/journal.pone.0194826>.
- (3) Gerich, J. E.; Charles, M. A.; Grodsky, G. M. Regulation of Pancreatic Insulin and Glucagon Secretion. *Annu. Rev. Physiol.* **1976**, *38*, 353–388. <https://doi.org/10.1146/annurev.ph.38.030176.002033>.
- (4) Aronoff, S. L.; Berkowitz, K.; Shreiner, B.; Want, L. Glucose Metabolism and Regulation: Beyond Insulin and Glucagon. *Diabetes Spectr.* **2004**, *17* (3), 183–190. <https://doi.org/10.2337/diaspect.17.3.183>.
- (5) Michael, M. D.; Kulkarni, R. N.; Postic, C.; Previs, S. F.; Shulman, G. I.; Magnuson, M. A.; Kahn, C. R. Loss of Insulin Signaling in Hepatocytes Leads to Severe Insulin Resistance and Progressive Hepatic Dysfunction. *Mol. Cell* **2000**, *6* (1), 87–97. [https://doi.org/10.1016/S1097-2765\(05\)00015-8](https://doi.org/10.1016/S1097-2765(05)00015-8).
- (6) Rosenstock, J.; Ferrannini, E. Euglycemic Diabetic Ketoacidosis: A Predictable, Detectable, and Preventable Safety Concern with SglT2 Inhibitors. *Diabetes Care* **2015**, *38* (9), 1638–1642. <https://doi.org/10.2337/dc15-1380>.
- (7) Drivsholm, T.; De Fine Olivarius, N.; Nielsen, A. B. S.; Siersma, V. Symptoms, Signs and Complications in Newly Diagnosed Type 2 Diabetic Patients, and Their Relationship to Glycaemia, Blood Pressure and Weight. *Diabetologia* **2005**, *48* (2), 210–214. <https://doi.org/10.1007/s00125-004-1625-y>.
- (8) Adams, A. G.; Krishna, R.; Bulusu, M.; Mukhitov, N.; Mendoza-Cortes, J. L.; Roper, M. G. Online Measurement of Glucose Consumption from HepG2 Cells Using an Integrated Bioreactor and Enzymatic Assay. **2021**, *21*, 53. <https://doi.org/10.1021/acs.analchem.8b05798>.
- (9) Quesada, I.; Tudurí, E.; Ripoll, C.; Nadal, Á. Physiology of the Pancreatic α -Cell and Glucagon Secretion: Role in Glucose Homeostasis and Diabetes. *J. Endocrinol.* **2008**, *199* (1), 5–19. <https://doi.org/10.1677/JOE-08-0290>.
- (10) Shackman, J. G.; Reid, K. R.; Dugan, C. E.; Kennedy, R. T. Dynamic Monitoring of Glucagon Secretion from Living Cells on a Microfluidic Chip. <https://doi.org/10.1007/s00216-012-5755-7>.
- (11) Roper, M. G.; Shackman, J. G.; Dahlgren, G. M.; Kennedy, R. T. Microfluidic Chip for Continuous Monitoring of Hormone Secretion from Live Cells Using an Electrophoresis-

- Based Immunoassay. *Anal. Chem.* **2003**, *75* (18), 4711–4717.
<https://doi.org/10.1021/ac0346813>.
- (12) Bandak, B.; Yi, L.; Roper, M. G. Microfluidic-Enabled Quantitative Measurements of Insulin Release Dynamics from Single Islets of Langerhans in Response to 5-Palmitic Acid Hydroxy Stearic Acid. *Lab Chip* **2018**, *18* (18), 2873–2882.
<https://doi.org/10.1039/c8lc00624e>.
- (13) Matveyenko, A. V.; Liuwantara, D.; Gurlo, T.; Kirakossian, D.; Dalla Man, C.; Cobelli, C.; White, M. F.; Copps, K. D.; Volpi, E.; Fujita, S.; Butler, P. C. Pulsatile Portal Vein Insulin Delivery Enhances Hepatic Insulin Action and Signaling. *Diabetes* **2012**, *61* (9), 2269–2279. <https://doi.org/10.2337/db11-1462>.
- (14) Rajkumar, S. V. The High Cost of Insulin in the United States: An Urgent Call to Action. *Mayo Clin. Proc.* **2020**, *95* (1), 22–28. <https://doi.org/10.1016/j.mayocp.2019.11.013>.
- (15) Boden, G.; Sargrad, K.; Homko, C.; Mozzoli, M.; Stein, T. P. Effect of a Low-Carbohydrate Diet on Appetite, Blood Glucose Levels, and Insulin Resistance in Obese Patients with Type 2 Diabetes.[Summary for Patients in *Ann Intern Med.* 2005 Mar 15;142(6):144; PMID: 15767614]. *Ann. Intern. Med.* **2005**, *142* (6), 403–411.
- (16) Philip E. Cryer, Stephen N. Davis, and H. S. Hypoglycemia in Diabetes. *Nurs. Clin. North Am.* **2017**, *52* (4), 565–574. <https://doi.org/10.1016/j.cnur.2017.07.006>.
- (17) Li, C.; Liu, C.; Nissim, I.; Chen, J.; Chen, P.; Doliba, N.; Zhang, T.; Nissim, I.; Daikhin, Y.; Stokes, D.; Yudkoff, M.; Bennett, M. J.; Stanley, C. A.; Insky, F. M. M.; Naji, A. Regulation of Glucagon Secretion in Normal and Diabetic Human Islets by γ -Hydroxybutyrate and Glycine. *J. Biol. Chem.* **2013**, *288* (6), 3938–3951.
<https://doi.org/10.1074/jbc.M112.385682>.
- (18) Morales, J.; Schneider, D. Hypoglycemia. *Am. J. Med.* **2014**, *127* (10), S17–S24.
<https://doi.org/10.1016/j.amjmed.2014.07.004>.
- (19) Lund, A.; Bagger, J. I.; Christensen, M.; Knop, F. K.; Vilsbøll, T. Glucagon and Type 2 Diabetes: The Return of the Alpha Cell. *Curr. Diab. Rep.* **2014**, *14* (12), 1–7.
<https://doi.org/10.1007/s11892-014-0555-4>.
- (20) Ritzel, R. A.; Veldhuis, J. D.; Butler, P. C. The Mass, but Not the Frequency, of Insulin Secretory Bursts in Isolated Human Islets Is Entrained by Oscillatory Glucose Exposure. *Am J Physiol Endocrinol Metab* **2005**, *290* (4), E750–E756.
<https://doi.org/10.1152/ajpendo.00381.2005>.
- (21) Brereton, M. F.; Iberl, M.; Shimomura, K.; Zhang, Q.; Adriaenssens, A. E.; Proks, P.; Spiliotis, I. I.; Dace, W.; Mattis, K. K.; Ramracheya, R.; Gribble, F. M.; Reimann, F.; Clark, A.; Rorsman, P.; Ashcroft, F. M. Reversible Changes in Pancreatic Islet Structure and Function Produced by Elevated Blood Glucose. *Nat. Commun.* **2014**, *5*.
<https://doi.org/10.1038/ncomms5639>.

- (22) Langerhans, P.; H. Morrison. Author (s): HYMEN SAYE Source : Bulletin of the Institute of the History of Medicine , Vol . 3 , No . 2 (FEBRUARY , Published by : The Johns Hopkins University Press Stable URL : [Http://Www.Jstor.Org/Stable/44437894](http://Www.Jstor.Org/Stable/44437894). **2018**, 3 (2), 165–167.
- (23) Sakai, K.; Matsumoto, K.; Nishikawa, T.; Suefuji, M.; Nakamaru, K.; Hirashima, Y.; Kawashima, J.; Shirotani, T.; Ichinose, K.; Brownlee, M.; Araki, E. Mitochondrial Reactive Oxygen Species Reduce Insulin Secretion by Pancreatic β -Cells. *Biochem. Biophys. Res. Commun.* **2003**, 300 (1), 216–222. [https://doi.org/10.1016/S0006-291X\(02\)02832-2](https://doi.org/10.1016/S0006-291X(02)02832-2).
- (24) Sharma, R. B.; Alonso, L. C. Lipotoxicity in the Pancreatic Beta Cell: Not Just Survival and Function, but Proliferation as Well? *Curr. Diab. Rep.* **2014**, 14 (6). <https://doi.org/10.1007/s11892-014-0492-2>.
- (25) Shackman, J. G.; Dahlgren, G. M.; Peters, J. L.; Kennedy, R. T. Perfusion and Chemical Monitoring of Living Cells on a Microfluidic Chip. *Lab Chip* **2005**, 5 (1), 56–63. <https://doi.org/10.1039/b404974h>.
- (26) Lang, D. A.; Matthews, D. R.; Burnett, M.; Turner, R. C. Brief, Irregular Oscillations of Basal Plasma Insulin and Glucose Concentrations in Diabetic Man. *Diabetes* **1981**, 30 (5), 435–439. <https://doi.org/10.2337/diab.30.5.435>.
- (27) Hruban, R. H.; Wilentz, R. E.; Kern, S. E. Genetic Progression in the Pancreatic Ducts. *Am. J. Pathol.* **2000**, 156 (6), 1821–1825. [https://doi.org/10.1016/S0002-9440\(10\)65054-7](https://doi.org/10.1016/S0002-9440(10)65054-7).
- (28) Brissova, M.; Fowler, M. J.; Nicholson, W. E.; Chu, A.; Hirshberg, B.; Harlan, D. M.; Powers, A. C. Assessment of Human Pancreatic Islet Architecture and Composition by Laser Scanning Confocal Microscopy. *J. Histochem. Cytochem.* **2005**, 53 (9), 1087–1097. <https://doi.org/10.1369/jhc.5C6684.2005>.
- (29) Murlin, J. R.; Clough, H. D.; Gibbs, C. B. F.; Stokes, A. M. Aqueous Extracts of Pancreas. *J. Biol. Chem.* **1923**, 56 (1), 253–296. [https://doi.org/10.1016/s0021-9258\(18\)85619-8](https://doi.org/10.1016/s0021-9258(18)85619-8).
- (30) Komjati, M.; Bratusch-Marrain, P.; Waldhäusl, W. Superior Efficacy of Pulsatile versus Continuous Hormone Exposure on Hepatic Glucose Production in Vitro. *Endocrinology* **1986**, 118 (1), 312–319. <https://doi.org/10.1210/endo-118-1-312>.
- (31) Cevc, G.; Gebauer, D.; Stieber, J.; Schätzlein, A.; Blume, G. Ultraflexible Vesicles, Transfersomes, Have an Extremely Low Pore Penetration Resistance and Transport Therapeutic Amounts of Insulin across the Intact Mammalian Skin. *Biochim. Biophys. Acta - Biomembr.* **1998**, 1368 (2), 201–215. [https://doi.org/10.1016/S0005-2736\(97\)00177-6](https://doi.org/10.1016/S0005-2736(97)00177-6).
- (32) Toft-Nielsen, M. B.; Madsbad, S.; Holst, J. J. The Effect of Glucagon-like Peptide I (GLP-I) on Glucose Elimination in Healthy Subjects Depends on the Pancreatic Glucoregulatory Hormones. *Diabetes* **1996**, 45 (5), 552–556. <https://doi.org/10.2337/diabetes.45.5.552>.

- (33) Hoang, D. T.; Matsunari, H.; Nagaya, M.; Nagashima, H.; Millis, J. M.; Witkowski, P.; Periwal, V.; Hara, M.; Jo, J. A Conserved Rule for Pancreatic Islet Organization. *PLoS One* **2014**, *9* (10), 1–9. <https://doi.org/10.1371/journal.pone.0110384>.
- (34) Svetlana Mojsov, Gordon C. Weir, J. F. H. Perfused Rat Pancreas . **1987**, *79* (2), 616–619.
- (35) Heinrich, G.; Gros, P.; Habener, J. F. Glucagon Gene Sequence. Four of Six Exons Separate Functional Domains of Rat Pre-Proglucagon. *J. Biol. Chem.* **1984**, *259* (22), 14082–14087. [https://doi.org/10.1016/s0021-9258\(18\)89859-3](https://doi.org/10.1016/s0021-9258(18)89859-3).
- (36) Almaça, J.; Molina, J.; Menegaz, D.; Pronin, A. N.; Tamayo, A.; Slepak, V.; Berggren, P. O.; Caicedo, A. Human Beta Cells Produce and Release Serotonin to Inhibit Glucagon Secretion from Alpha Cells. *Cell Rep.* **2016**, *17* (12), 3281–3291. <https://doi.org/10.1016/j.celrep.2016.11.072>.
- (37) D’Alessio, D. The Role of Dysregulated Glucagon Secretion in Type 2 Diabetes. *Diabetes, Obes. Metab.* **2011**, *13* (SUPPL. 1), 126–132. <https://doi.org/10.1111/j.1463-1326.2011.01449.x>.
- (38) Cho, K. J.; Wilcox, C. W.; Reuter, S. R. Of the Pancreas. *Adv. Surg.* **2009**, *43* (1), 269–282.
- (39) Magnusson, I.; Rothman, D. L.; Gerard, D. P.; Katz, L. D.; Shulman, G. I. Contribution of Hepatic Glycogenolysis to Glucose Production in Humans in Response to a Physiological Increase in Plasma Glucagon Concentration. *Diabetes* **1995**, *44* (2), 185–189. <https://doi.org/10.2337/diabetes.44.2.185>.
- (40) Adeva-Andany, M. M.; González-Lucán, M.; Donapetry-García, C.; Fernández-Fernández, C.; Ameneiros-Rodríguez, E. Glycogen Metabolism in Humans. *BBA Clin.* **2016**, *5*, 85–100. <https://doi.org/10.1016/j.bbacli.2016.02.001>.
- (41) Leloup, C.; Tourrel-Cuzin, C.; Magnan, C.; Karaca, M.; Castel, J.; Carneiro, L.; Colombani, A. L.; Ktorza, A.; Casteilla, L.; Pénicaud, L. Mitochondrial Reactive Oxygen Species Are Obligatory Signals for Glucose-Induced Insulin Secretion. *Diabetes* **2009**, *58* (3), 673–681. <https://doi.org/10.2337/db07-1056>.
- (42) Hers, H. G.; Hue, L. Gluconeogenesis And. **1983**.
- (43) Unger, B. R. H.; Eisentraut, A. M.; McCall, M. S.; Leonard, L. GLUCAGON ANTIBODIES AND AN IMMUNOASSAY FOR GLUCAGON * Despite Extensive Knowledge of the Amino Acid Composition of Beef-Pork Glucagon , and of the Physiologic Changes Induced by Its Administration to Animals and Man , the Role of Glucagon in the Homeostat. **1961**, 1280–1289.
- (44) Lomasney, A. R.; Yi, L.; Roper, M. G. Simultaneous Monitoring of Insulin and Islet Amyloid Polypeptide Secretion from Islets of Langerhans on a Microfluidic Device. *Anal. Chem.* **2013**, *85* (16), 7919–7925. <https://doi.org/10.1021/ac401625g>.

- (45) Michael Roper, S. G.; Schrell, A. M.; Mukhitov, N.; Yi, L.; Adablah, J. E.; Menezes, J.; Roper, M. G. As Featured in: Online Fluorescence Anisotropy Immunoassay for Monitoring Insulin Secretion from Islets of Langerhans †. **2017**. <https://doi.org/10.1039/c6ay02899c>.
- (46) Lundin, K.; Blomberg, K.; Nordström, T.; Lindqvist, C. Development of a Time-Resolved Fluorescence Resonance Energy Transfer Assay (Cell TR-FRET) for Protein Detection on Intact Cells. *Anal. Biochem.* **2001**, *299* (1), 92–97. <https://doi.org/10.1006/abio.2001.5370>.
- (47) Bunt, G.; Wouters, F. S. FRET from Single to Multiplexed Signaling Events. *Biophys. Rev.* **2017**, *9* (2), 119–129. <https://doi.org/10.1007/s12551-017-0252-z>.
- (48) Clapp, A. R.; Medintz, I. L.; Mattoussi, H. Förster Resonance Energy Transfer Investigations Using Quantum-Dot Fluorophores. *ChemPhysChem* **2006**, *7* (1), 47–57. <https://doi.org/10.1002/cphc.200500217>.
- (49) Zal, T.; Gascoigne, N. R. J. Photobleaching-Corrected FRET Efficiency Imaging of Live Cells. *Biophys. J.* **2004**, *86* (6), 3923–3939. <https://doi.org/10.1529/biophysj.103.022087>.
- (50) Pisania, A.; Weir, G. C.; Neil, J. J. O.; Omer, A.; Tchishopashvili, V.; Lei, J.; Colton, C. K.; Bonner-weir, S. Quantitative Analysis of Cell Composition and Purity of Human Pancreatic Islet Preparations. **2010**, *90* (November), 1661–1675. <https://doi.org/10.1038/labinvest.2010.124>.
- (51) Ravier, M. A.; Daro, D.; Roma, L. P.; Jonas, J. C.; Cheng-Xue, R.; Schuit, F. C.; Gilon, P. Mechanisms of Control of the Free Ca²⁺ Concentration in the Endoplasmic Reticulum of Mouse Pancreatic β -Cells: Interplay with Cell Metabolism and [Ca²⁺]_c and Role of SERCA2b and SERCA3. *Diabetes* **2011**, *60* (10), 2533–2545. <https://doi.org/10.2337/db10-1543>.
- (52) Bevacqua, R. J.; Dai, X.; Lam, J. Y.; Gu, X.; Friedlander, M. S. H.; Tellez, K.; Miguel-Escalada, I.; Bonàs-Guarch, S.; Atla, G.; Zhao, W.; Kim, S. H.; Dominguez, A. A.; Qi, L. S.; Ferrer, J.; MacDonald, P. E.; Kim, S. K. CRISPR-Based Genome Editing in Primary Human Pancreatic Islet Cells. *Nat. Commun.* **2021**, *12* (1), 1–12. <https://doi.org/10.1038/s41467-021-22651-w>.
- (53) Schrell, A. M.; Mukhitov, N.; Yi, L.; Wang, X.; Roper, M. G. Microfluidic Devices for the Measurement of Cellular Secretion. <https://doi.org/10.1146/annurev-anchem-071114-040409>.
- (54) Yi, L.; Bandak, B.; Wang, X.; Bertram, R.; Roper, M. G. Dual Detection System for Simultaneous Measurement of Intracellular Fluorescent Markers and Cellular Secretion. *Anal. Chem.* **2016**, *88* (21), 10368–10373. <https://doi.org/10.1021/acs.analchem.6b02404>.
- (55) Castiello, F. R.; Heileman, K.; Tabrizian, M. Lab on a Chip CRITICAL REVIEW Microfluidic Perfusion Systems for Secretion Fingerprint Analysis of Pancreatic Islets: Applications, Challenges and Opportunities. **2014**, *16*, 409. <https://doi.org/10.1039/c5lc01046b>.

- (56) Shaikh Mohammed, J.; Wang, Y.; Harvat, T. A.; Oberholzer ab, J.; Eddington, D. T. Microfluidic Device for Multimodal Characterization of Pancreatic Islets. <https://doi.org/10.1039/b809590f>.
- (57) Dishinger, J. F.; Kennedy, R. T. Serial Immunoassays in Parallel on a Microfluidic Chip for Monitoring Hormone Secretion from Living Cells. *Anal. Chem.* **2007**, *79* (3), 947–954. <https://doi.org/10.1021/ac061425s>.
- (58) Easley, C. J.; Rocheleau, J. V.; Head, W. S.; Piston, D. W. Quantitative Measurement of Zinc Secretion from Pancreatic Islets with High Temporal Resolution Using Droplet-Based Microfluidics. <https://doi.org/10.1021/ac9017692>.
- (59) Godwin, L. A.; Pilkerton, M. E.; Deal, K. S.; Wanders, D.; Judd, R. L.; Easley, C. J. Passively Operated Microfluidic Device for Stimulation and Secretion Sampling of Single Pancreatic Islets. <https://doi.org/10.1021/ac201598b>.
- (60) Lenguito, G.; Chaimov, D.; Weitz, J. R.; Rodriguez-Diaz, R.; Rawal, S. A. K.; Tamayo-Garcia, A.; Caicedo, A.; Stabler, C. L.; Buchwald, P.; Agarwal, A. Resealable, Optically Accessible, PDMS-Free Fluidic Platform for Ex Vivo Interrogation of Pancreatic Islets. *Lab Chip* **2017**, *17* (5), 772–781. <https://doi.org/10.1039/c6lc01504b>.
- (61) Walker, J. T.; Haliyur, R.; Nelson, H. A.; Ishahak, M.; Poffenberger, G.; Aramandla, R.; Reihsmann, C.; Luchsinger, J. R.; Saunders, D. C.; Wang, P.; Garcia-Ocaña, A.; Bottino, R.; Agarwal, A.; Powers, A. C.; Brissova, M. TECHNICAL ADVANCE Integrated Human Pseudoislet System and Microfluidic Platform Demonstrate Differences in GPCR Signaling in Islet Cells. **2020**. <https://doi.org/10.1172/jci.insight.137017>.
- (62) Yi, L.; Wang, X.; Dhumpa, R.; Schrell, A. M.; Mukhitov, N.; Roper, M. G. From Chip-in-a-Lab to Lab-on-a-Chip: Towards a Single Handheld Electronic System for Multiple Application-Specific Lab-on-a-Chip (ASLOC). **2014**, *15*, 823. <https://doi.org/10.1039/c4lc01360c>.
- (63) Yi, L.; Wang, X.; Bethge, L.; Klussmann, S.; Roper, M. G. Noncompetitive Affinity Assays of Glucagon and Amylin Using Mirror-Image Aptamers as Affinity Probes. *Analyst* **2016**, *141* (6), 1939–1946. <https://doi.org/10.1039/c5an02468d>.
- (64) Leng, W.; Evans, K.; Roper, M. G. A Microfluidic Platform Integrating Pressure-Driven and Electroosmotic-Driven Flow with Inline Filters for Affinity Separations. *Anal. Methods* **2019**, *11* (45), 5768–5775. <https://doi.org/10.1039/c9ay01758e>.
- (65) Heyduk, E.; Moxley, M. M.; Salvatori, A.; Corbett, J. A.; Heyduk, T. Homogeneous Insulin and C-Peptide Sensors for Rapid Assessment of Insulin and C-Peptide Secretion by the Islets. *Diabetes* **2010**, *59* (10), 2360–2365. <https://doi.org/10.2337/db10-0088>.
- (66) Li, X.; Hu, J.; Easley, C. J. Automated Microfluidic Droplet Sampling with Integrated, Mix-and-Read Immunoassays to Resolve Endocrine Tissue Secretion Dynamics. *Lab Chip* **2018**, *18* (19), 2926–2935. <https://doi.org/10.1039/c8lc00616d>.

- (67) Henquin, J. C. The Challenge of Correctly Reporting Hormones Content and Secretion in Isolated Human Islets. *Mol. Metab.* **2019**, *30* (October), 230–239. <https://doi.org/10.1016/j.molmet.2019.10.003>.
- (68) Donohue, M. J.; Filla, R. T.; Steyer, D. J.; Eaton, W. J.; Roper, M. G. Rapid Liquid Chromatography-Mass Spectrometry Quantitation of Glucose-Regulating Hormones from Human Islets of Langerhans. *J. Chromatogr. A* **2021**, *1637*, 461805. <https://doi.org/10.1016/j.chroma.2020.461805>.
- (69) Sankar, K. S.; Green, B. J.; Crocker, A. R.; Verity, J. E.; Altamentova, S. M.; Rocheleau, J. V. Culturing Pancreatic Islets in Microfluidic Flow Enhances Morphology of the Associated Endothelial Cells. *PLoS One* **2011**, *6* (9), 1–11. <https://doi.org/10.1371/journal.pone.0024904>.
- (70) Gutscher, M.; Pauleau, A. L.; Marty, L.; Brach, T.; Wabnitz, G. H.; Samstag, Y.; Meyer, A. J.; Dick, T. P. Real-Time Imaging of the Intracellular Glutathione Redox Potential. *Nat. Methods* **2008**, *5* (6), 553–559. <https://doi.org/10.1038/nmeth.1212>.
- (71) Gerber, P. A.; Rutter, G. A. The Role of Oxidative Stress and Hypoxia in Pancreatic Beta-Cell Dysfunction in Diabetes Mellitus. *Antioxidants Redox Signal.* **2017**, *26* (10), 501–518. <https://doi.org/10.1089/ars.2016.6755>.
- (72) Zhou, Y. P.; Grill, V. E. Long-Term Exposure of Rat Pancreatic Islets to Fatty Acids Inhibits Glucose-Induced Insulin Secretion and Biosynthesis through a Glucose Fatty Acid Cycle. *J. Clin. Invest.* **1994**, *93* (2), 870–876. <https://doi.org/10.1172/JCI117042>.
- (73) Syed, I.; Lee, J.; Moraes-Vieira, P. M.; Donaldson, C. J.; Sontheimer, A.; Aryal, P.; Wellenstein, K.; Kolar, M. J.; Nelson, A. T.; Siegel, D.; Mokrosinski, J.; Farooqi, I. S.; Zhao, J. J.; Yore, M. M.; Peroni, O. D.; Saghatelian, A.; Kahn, B. B. Palmitic Acid Hydroxystearic Acids Activate GPR40, Which Is Involved in Their Beneficial Effects on Glucose Homeostasis. *Cell Metab.* **2018**, *27* (2), 419-427.e4. <https://doi.org/10.1016/j.cmet.2018.01.001>.
- (74) Reissaus, C. A.; Piñeros, A. R.; Twigg, A. N.; Orr, K. S.; Conteh, A. M.; Martinez, M. M.; Kamocka, M. M.; Day, R. N.; Tersey, S. A.; Mirmira, R. G.; Dunn, K. W.; Linnemann, A. K. A Versatile, Portable Intravital Microscopy Platform for Studying Beta-Cell Biology In Vivo. *Sci. Rep.* **2019**, *9* (1), 1–11. <https://doi.org/10.1038/s41598-019-44777-0>.
- (75) Eaton, W. J.; Roper, M. G. A Microfluidic System for Monitoring Glucagon Secretion from Human Pancreatic Islets of Langerhans. *Anal. Methods* **2021**. <https://doi.org/10.1039/D1AY00703C>.
- (76) Dhumpa, R.; Truong, T. M.; Wang, X.; Bertram, R.; Roper, M. G. Negative Feedback Synchronizes Islets of Langerhans. *Biophys. J.* **2014**, *106* (10), 2275–2282. <https://doi.org/10.1016/j.bpj.2014.04.015>.
- (77) Bindokas, V. P.; Kuznetsov, A.; Sreenan, S.; Polonsky, K. S.; Roe, M. W.; Philipson, L. H. Visualizing Superoxide Production in Normal and Diabetic Rat Islets of Langerhans. *J.*

- Biol. Chem.* **2003**, 278 (11), 9796–9801. <https://doi.org/10.1074/jbc.M206913200>.
- (78) Cabrera, O.; Berman, D. M.; Kenyon, N. S.; Ricordi, C.; Berggren, P.-O.; Caicedo, A. The Unique Cytoarchitecture of Human Pancreatic Islets Has Implications for Islet Cell Function. *Proc. Natl. Acad. Sci.* **2006**, 103 (7), 2334–2339. <https://doi.org/10.1073/pnas.0510790103>.
- (79) Adablah, J. E.; Wang, Y.; Donohue, M.; Roper, M. G. Profiling Glucose-Stimulated and M3 Receptor-Activated Insulin Secretion Dynamics from Islets of Langerhans Using an Extended-Lifetime Fluorescence Dye. *Anal. Chem.* **2020**, 92 (12), 8464–8471. <https://doi.org/10.1021/acs.analchem.0c01226>.
- (80) Stubenrauch, K.; Wessels, U.; Essig, U.; Kowalewsky, F.; Vogel, R.; Heinrich, J. Characterization of Murine Anti-Human Fab Antibodies for Use in an Immunoassay for Generic Quantification of Human Fab Fragments in Non-Human Serum Samples Including Cynomolgus Monkey Samples. *J. Pharm. Biomed. Anal.* **2013**, 72, 208–215. <https://doi.org/10.1016/j.jpba.2012.08.023>.
- (81) Ocvirk, G.; Tang, T.; Harrison, D. J. Optimization of Confocal Epifluorescence Microscopy for Microchip-Based Miniaturized Total Analysis Systems. *Analyst* **1998**, 123 (7), 1429–1434. <https://doi.org/10.1039/a800153g>.
- (82) Minsky, M. Memoir on Inventing the Confocal Scanning Microscope. *Scanning* **1988**, 10 (4), 128–138. <https://doi.org/10.1002/sca.4950100403>.

BIOGRAPHICAL SKETCH

Wesley Eaton received his Bachelor of Science degree in Chemical Science from Florida State University in Tallahassee, FL in 2016. In fall of the same year, he enrolled in the Department of Chemistry and Biochemistry Ph.D. program at Florida State University in Tallahassee, FL, where he joined the Roper Laboratory. His research interests include developing optical detection systems, using microfluidic methods and immunoassay techniques to measure insulin and glucagon release dynamics from human islets of Langerhans, and how the secretion rates change under various glucose conditions. He received his Ph.D. in Analytical Chemistry in fall 2021.